Probabilistic Dynamics of Wind Excitation on Glass Facade

Dem Fachbereich Bauingenieurwesen und Geodäsie
der Technischen Universität Darmstadt
zur Erlangung des akademischen Grades eines
Doktor-Ingenieurs (Dr.-Ing.)
genehmigte

DISSERTATION

vorgelegt von
Yukako Nakagami
aus Chiba, Japan

D17

Darmstadt 2003

Referent:	Prof. Dr.-Ing. J.-D. Wörner
Korreferent:	Prof. Dr.-Ing. U. C. E. Zanke
Tag der Einreichung:	22. Januar 2003
Tag der Prüfung:	3. April 2003

Zusammenfassung

In den letzten Jahren sind viele Gebäude mit Glasfassaden gebaut worden. Durch diese Tendenz sind neue Glasmaterialien, Lagerung- und Tragsystem entwickelt worden. Wind ist eine der Hauptlasten auf Glasfassaden. Die Windlast ist eine dynamische Last, jedoch sind die dynamischen Eigenschaften der neuen Glasmaterialien noch nicht bekannt. Außerdem besitzt das Material Glas eine niedrige Dämpfung. Auf die Gefahr von Schwingungen in Glasfassaden wird hingewiesen.
Das erste Ziel dieser Arbeit ist es, die dynamischen Eigenschaften der Glasfassade und Windlast zu erhalten.
Zunächst sind die dynamischen Eigenschaften des Windes in der Atmosphäre untersucht worden. Der Geschwindigkeitsdruck wurde numerisch reproduziert. Danach wurden die Schwingungen eines Glasfassadenelements unter wechselnden Windlasten im Zeitbereich simuliert. Die Simulation der Glasfassade wurde anhand von Einscheiben-Sicherheits-Glas (ESG) Elementen mit einer Fläche von 2,5-6,0 m^2 durchgeführt. Die Glasscheiben wurden entlang des Randes liniengelagert oder punktgelagert. Die Ergebnisse wurden mit Hilfe der Fast-Fourier-Transformation vom Zeit- in den Frequenzbereich überführt. Im Spektrum der Verformung eines punktgelagerten, großflächige Fassadenelements lässt sich ein Resonanzeffekt bei der ersten Eigenfrequenz erkennen.

Aus den Ergebnissen im Zeitbereich wurde auf die, durch die Bewegung der Glasscheibe entstehende, induzierte Windkraft rückgeschlossen. Die gesamte Windkraft setzt sich zusammen aus der wechselnden Windkraft und der von der Bewegung induzierten Kraft.

Das Problem der Ermüdung des Glasmaterials macht eine Ermüdungsanalyse erforderlich. Für eine Ermüdungsanalyse ist die Kenntnis der Wöhlerlinie und der Lastkollektive erforderlich. Das nächste Ziel der Forschung ist es, die Lastkollektive für die Lebensdauer einer Fassade zu bestimmen. Es gibt einige Methoden, um von einer zeitlichen unregelmäßigen Belastung auf ein Lastkollektiv zu schließen. Im Rahmen dieser Arbeit wurde eine neue Methode entwickelt, um aus einem Spektrum ein Lastkollektiv zu bestimmen. Zunächst wurden Lastkollektive, die durch eine zehnminütige variable Windlast unter bestimmten Windbedingungen hervorgerufen wurden, berechnet.
Danach wurde ein Lastkollektiv, das die lebenslange Windbelastung beschreibt, wahrscheinlichkeitstheoretisch berechnet.

Die Weibull-Verteilung beschreibt die Wahrscheinlichkeitsverteilung der mittleren Windgeschwindigkeit sehr gut. Mit den einzelnen Lastkollektiven und deren jeweiliger Wahrscheinlichkeit wurde das Lastkollektiv für eine lebenslange (50 Jahre) Windbelastung bestimmt. Mit dieser Methode sind Lastkollektive für Fassaden in 20 und 50 m Höhe für Gebäude in Frankfurt und Hamburg berechnet worden.

Table of Contents

List of Figures

List of Tables

1 Introduction

1.1 Object of the Study

In recent years many structures in which glass material is used to a great extent, such as the Leipzig Exhibition Center and the New German Parliament, have been constructed. This tendency is clear specially in Germany where the number of daylight hours are few in winter and the sunshine in summer is not very strong. Hence there is a need to introduce sunlight into buildings and the demand for structures filled with glass facades will continue to grow in the future.

Wind load is a dynamic load which acts continuously during the lifetime of the structure.
There are many problems of wind effect for the structure. Vibration for long span bridges and skyscrapers is serious problem because the wind and vortex around a building is a danger for facades and passers. However, most of the wind damages are on roofs or facade elements, especially in turbulent weather like a storm, hurricane and typhoon. For example, in August 1992, many glass windows were broken in many of buildings by Hurricane Andrew because of high local pressure[1.1]. As an example of recent years, the typhoon York attacked Hong Kong in September 1999 and caused serious damage to the glass claddings of tall buildings[1.2].

For a long time many studies about the wind dynamic loads on structures and interaction between structure and air have been performed. But these studies are mainly about long span structures like bridges or skyscrapers. About facades, because of the light weight and the high frequency of them, the dynamic problems have almost not been discussed.

In some construction codes, methods to estimate the design wind load are classified according to facade elements and structures. In addition to this, methods for structures are further classified according to structures that are sensitive to dynamic force and not sensitive to dynamic force. It is only in the sensitive case, where the structure has a relatively low natural frequency and apparent stiffness, that the design wind force includes the additional aero-force induced by aero elastic vibration. In the non-sensitive case, the quasi static wind load is calculated based on the view that the maximum instantaneous wind velocity during the lifetime of the structure gives the maximum wind pressure.
For a facade element the vortex that induces extreme negative pressures is taken into account, but not the aerodynamic effect, and the quasi static method is carried out in the case of a structure that is not sensitive to the vibration.

However in spite of these codes, accidents such as failure of glass happen sometimes in Europe. Industrial problems such as material quality or technical problems for example unknown material characters can also be a reason. It is a big problem that the dynamic effect of the wind, such as resonance or additional aero dynamic force on facade elements, are not made clear because of historical background. Actually, the “dynamic” wind load on any

structures contains the dynamics of natural wind and dynamics due to the movement of structure. Now the need to study the dynamic action of wind load on glass is pointed out.

In addition, glass has no plastic regime and it has dynamic and static fatigue problems.
It is known that glass strength is lowered in repeated load. This phenomenon is called fatigue strength and its character strongly depends on the character of the repeating load. Thus, to estimate the fatigue of the material, it is necessary to obtain the loading-cycle and loading value.

A counting method of dynamic loading-cycle has been developed in the field of structures, vehicles and streets. However the loading-cycles, which are counted from time series dynamic load, do not reflect the frequency character of loading[1.3].
In the section for the slender structures like antenna musts or chimneys of DIN, one can find a method to count the loading-cycles of wind load, whose frequency is close to the natural frequency of a structure, during the lifetime of the structure[1.4]. With this method, however, one calculates only the loading-cycle of resonance component in wind load. It is necessary to count the loading-cycle taking the wide range of the frequency of wind component into account.

Fatigue effect of glass is large. It is known that the fatigue is caused by the corrosion in cracks on the surface of a glass. For the estimation of the fatigue of glass, it is necessary to investigate the wind loading-cycle and the value of loading exactly by using probabilistic approach.

Glass that is used as a facade element is often treated lightly compared with the structure system at the design. For the facade element, problems of dynamic effect and fatigue under the condition of long-term loading have not been investigated intensively. In many cases, failures in strong wind occur on facade elements and the failures introduce the next failure. In accordance of the shift of the design method, i.e, from the allowable design method to the reliability design method, the need to study the safety of facade elements is increasing.

1.2 Background

Regarding the wind load that acts on structures, Newton had already indicated that the wind load is proportional to the square of wind velocity[1.5]. Wind tunnel tests began at the beginning of the 20^{th} century. Many skyscrapers were built in New York in 1930´s and for most of them wind tunnel tests were carried out. However the tunnel tests at that time were under the constant aero flow and the wind load was recognized as a static load. In 1940, the accident of the Tacoma bridge, a 4-month old steel suspension, happened in the USA. After the accident, the importance of the dynamics of the wind load and the vibration of structure was recognized and studies about interaction between the wind and the air were started[1.6].
Vibrations of the structure are explained as phenomena like flutter, vortex induced vibration, buffeting and galloping. In these phenomenon, aero flow is disturbed by the structure and brings new dynamic load and the vibration of the structure produces an additional dynamic forces[1.7],[1.8]. Such dynamic forces, which are induced by the interaction between the

structure and air, are called unsteady aerodynamic forces. In particular an aero force by the motion of a structure is called motion-induced wind load.

In the 60´s, the importance of the turbulence in the natural wind was also recognized. Natural turbulence of wind was analyzed based on the statistic and probabilistic theory. Davenport developed the gust factor[1.9]. Few spectrums of the wind velocity were indicated at this time.

For the facade, the vortex shedding is recognized as a serious problem because it causes high negative local pressure. The vortex occurs very locally on a building surface and many measurements have been done on the surface of a building [1.10][1.11][1.12]. In these measurements the distribution of the maximum wind pressure coefficients on the surface of the structure is considered but there are few researches about the dynamic characters of the local pressure. Suresh and Stathopoulos measured the time series local pressure under a Hurricane and made a statistical analysis of the data[1.13].
These studies are reflected in the construction codes. Both the Eurocode and the SIA have a methods to estimate the wind loads on facade elements with different surface areas and on the different form and size of buildings[1.14][1.15].
But these studies consider the interaction between the building and air, but not between the facade and air. The problem of the vibration of the facade itself has not been discussed so far.

There are many references to glass material and glass facades. But there are few studies that focus on the dynamic character of glass. It is known that glass material has a strong fatigue effect and the strength depends on the loading. Generally the strength of a material strongly depends on the character of the loading. The studies about repeating load and the fatigue are developed in the field of mechanics[1.3][1.16].
There are a few counting methods of the loading-cycle from a random force[1.17][1.18]. Regarding the wind loading, there are studies of the loading-cycle under hurricane[1.19]. In the DIN 4131, the method is presented to count the loading-cycles of critical wind velocity for towers[1.4].

Until now there is no complete study of the fatigue of the glass under wind cycling load. For the estimation of the glass fatigue, it is necessary to analyze the wind load theoretically and obtained the suitable loading-cycle model.

1.3 Reference

[1.1] Minor, Joseph E. “Windborne debris and the building envelope”, Journal of Wind Engineering and Industrial Aerodynamics 53, 1994

[1.2] Hong Kong Observatory “Reports on the Typhoon”, http://www.weather.gov.hk/index.htm, last updated 6. July 2000

[1.3] Radaj, Dieter “Ermüdungsfestigkeit”, Springer-Verlag, 1995

[1.4] DIN 4131, “ Steel radio towers and masts ”, Nov. 1991 [1.German code]

[1.5] Davenport, A. G. The Interaction of Wind and Structures, Ch.12, Engineering Metheorolgy ed. By E.J. Plate, Elsevier, 1982

[1.6] Farquharson, E.B. Aerodynamic Stability of Suspension Bridges, a report of an investigation, the structural research laboratory, Washington University, 1950

[1.7] Rosemeier, G. “Winddruckprobleme bei Bauwerken”, Springer-Verlag, 1976

[1.8] Simiu, Emil and Scanlan, Robert H. “Wind effects on structures. - 2. ed. ” - New York Wiley, 1986

[1.9] Davenport, A.G. “Gust loading factor”, Journal of the Structural Division, ASCE, 1967

[1.10] Bienkiewicz, B. and Tamura, Y. “proper orthogonal decomposition and reconstruction of multi-channel roof pressure”, Journal of Wind Engineering and Industrial Aerodynamics 54&55, 1995

[1.11] Kasperski, M.; Koss, H. and Sahlmen, J. “BEATRICE Joint Project: Wind action on low-rise buildings” Journal of Wind Engineering and Industrial Aerodynamics 64, 1996

[1.12] Wiik, T. and Hansen, E.W.M. “The assessment of wind loads on roof overhang of low-rise buildings”, Journal of Wind Engineering and Industrial Aerodynamics 67&68, 1997

[1.13] Suresh Kummar, K. amd Stathopoulos, T. “Wind Loads on Low Building Roofs: a Stochastic Perspective”, Journal of Structural Engineering, ASCE August 2000

[1.14] EUROCODE 1 ENV 1991-2-4, “ Base of Design and Actions on Structures, Part 2.4 Wind Actions ”,1995

[1.15] SIA 160 “Einwirkung auf Tragwerke 406 Wind”, Schweizerischer Ingenieur- und Architekten-Verein, 1989

[1.16] Gerhardt, Hans-Christian “Zur Betriebsfestigkeit im Stahlbeton-und Spannbetonbau”, Dissertation vom Fachbereich Bauingenieurwesen der Technische Universität Darmstadt, 1984

[1.17] Dowling, N. E. [1.1972]. “Fatigue failure predictions for complicated stress-strain histories,” Journal of Materials 7: pp.71-78

[1.18] Matsuishi, M. and Endo, T. “Fatigue of metals subjected to varying stress”, Japan Sociery of Mechanical Engineers Meeting, Fukuoka, 1968

[1.19] Lechford, C. W. and Scott Norville. H. “Wind Pressure loading-cycles for wall cladding during hurricanes”, Journal of Wind Engineering and Industrial Aerodynamics 53, 1994

2 Wind Profile

2.1 Natural Wind

The air is moving and this movement is called natural wind. Wind is generated by various forces, from the global atmospheric circulation to the local geographical situation. In this section, the character of the natural wind is explained in the meteorological and geographical viewpoint.

2.1.1 Wind Climate

Atmospheric motion usually takes place in such a way that different patterns of motion are mutually independent both in time and in space. The patterns of atmospheric motion range from turbulence to local weather system and large planetary waves, which circumvent the entire globe and have a lifetime of several days. The orders of magnitude in space and time for different patterns of motion in the atmosphere are shown in Fig. 2.1.

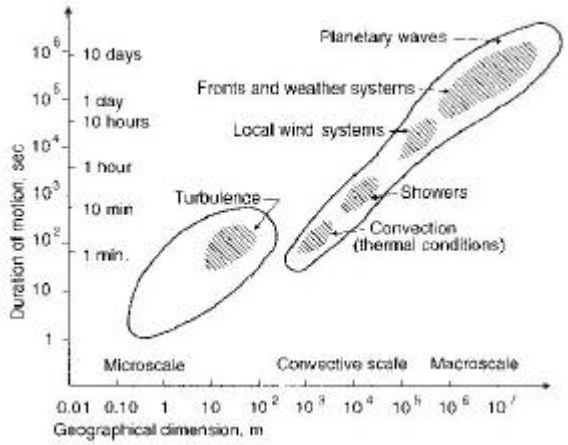

Fig. 2.1 Patterns of motion in the atmosphere
source: Dyrbye and Hansen [3.1]

Fig. 2.2 shows the Van der Hoven spectrum, that is made based on the measurement at about 100m height[2.1]. The spectrum has peaks at periods of 4 to 5 days and 1 to 2 minutes. The spectrum value in periods between approximately 10 minutes and about 5-10 hours is very low. This is referred to as a spectral gap. The first peak at periods of 4 to 5 days is thought to be due to wind climate by the entire globe scale atmosphere movement and the second peak at periods of 1-2 minutes is due to the turbulence in the atmospheric boundary layer. Both phenomena are independent and should be treated separately.
In the next section the turbulent wind in the atmospheric boundary layer, that brings the vibration problem on structures and cladding of the structures is described.

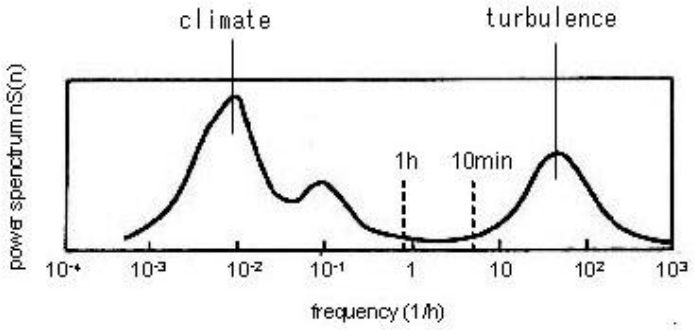

Fig. 2.2 Hoven spectrum for wind velocity

2.1.2 Mean Wind Velocity

Wind flow is turbulent due to the friction caused as it passes over surface terrain. A turbulent wind flow varies in a complex, random way both in space and time. The momentary velocity is described as the sum of a mean velocity and a fluctuating velocity. Fig. 2.3 shows a history of wind velocity, which varies in time.

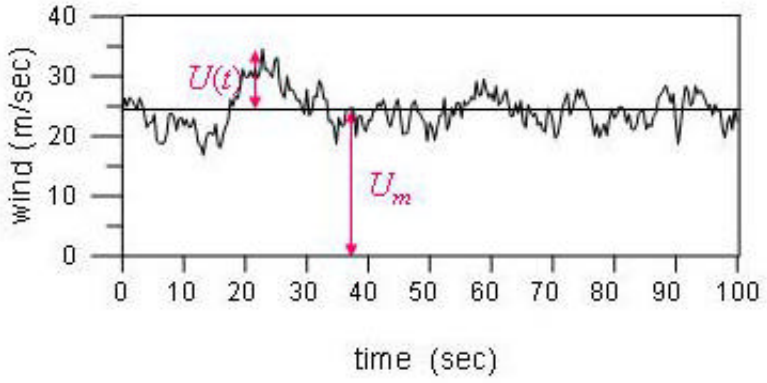

Fig. 2.3 Time series of fluctuating wind velocity

Mean wind velocity can be supposed stationary over 10 minutes. Usually 10-minute observed period is applied for calculating mean wind velocities. Wind is characterized by the mean wind velocity and the additional turbulence.

Wind velocity increases with the height above terrain in the atmospheric boundary layer. The terrain is expressed as the roughness length z_0. z_0 is interpreted as the size of a characteristic vortex, which is formed as a result of friction between air and the ground surface [2.2]. z_0 is the height above ground at which the mean wind velocity is zero.(see Fig. 2.4) In Eurocode 1 the roughness class is introduced[2.3]. Classification of the roughness class in the Eurocode is shown in Table 2.1.1.

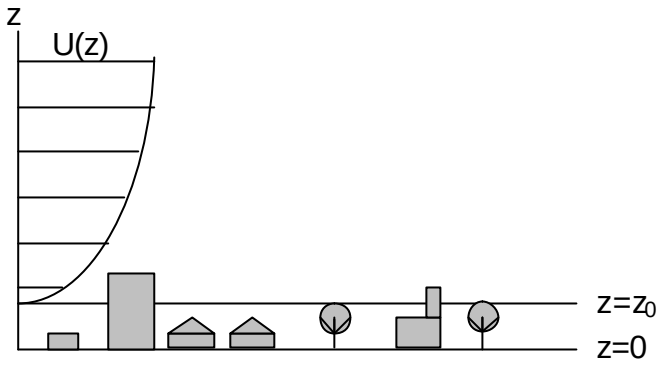

Fig. 2.4 Roughness length and increase of mean wind velocity as height

Mean wind velocity according to height

Mean wind velocities varies along the height and few mathematical models have been suggested. Generally mean wind velocities increase with height. Near to the ground in an urban area the mean wind velocity is smaller than that in an open place.

Davenport model

Davenport suggested the power-law profile[2.1]. This model is often used because of the simplicity. In the model the mean wind velocity at the height of z above ground is expressed as :

$$U(z) = U_{bas}\left(\frac{z}{z_{bas}}\right)^{a} \tag{2.1}$$

where U_{bas} is the reference wind velocity (see section 2.1.3.), z is the reference height (usually 10m) and a is the exponent that is shown in table 2.1.1.

Eurocode

Eurocode 1 states that the mean wind velocity varies according to height z above ground as follows:

$$U(z) = U_{bas} k_T \ln\left(\frac{z}{z_0}\right) \qquad \text{if } z_{min} = z = 200\text{m}$$
$$U(z) = U(z_{\min}) \qquad \text{if } z < z_{min} \tag{2.2}$$

where k_T is a terrain factor and the factor is set for each roughness class and z_{min} is a minimum height, under which the mean wind velocity does not increase. k_T and z_{min} are set in Eurocode and shown in Table. 2.1.1.

Fig. 2.5 shows the mean wind velocity along the height of the Davenport´s model and according to Eurocode.

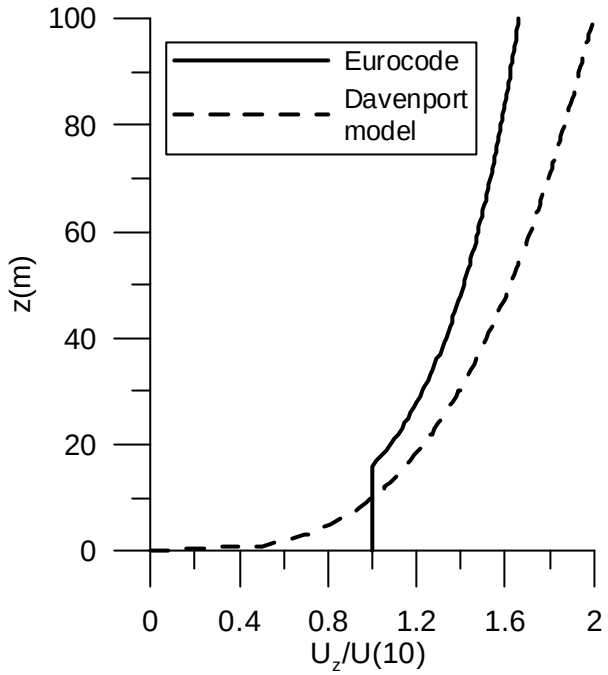

Fig. 2.5 Mean wind velocity along height by Davenport model and Eurocode urban area, U_{ref} is 10m/s

Table 2.1 Roughness category and related parameters according to Eurocode

	roughness class	z_0 [m]	k_T	z_{min} [m]	a
I	rough, open sea, lakes with at least 5 km fetch upwind and smooth flat country without obstacles	0.01	0.17	2	0.12
II	farmland with boundary hedges, occasional small farm structures, house or trees	0.05	0.19	4	0.16
III	suburban or industrial areas and permanent forests	0.3	0.22	8	0.22
IV	urban areas in which at least 15% of the surface is covered by building with an average height exceeding 15m	1	0.24	16	0.3

2.1.3 Extreme Wind

The statistical analysis of historical data was performed on recorded wind speed. The generalized extreme value distribution was suggested by Jenkinson in 1955 [2.4]. The probability distribution function of the maximum wind velocity $F_U(U)$ is given by:

$$F_U(U) = \exp\left\{-\left[1-\frac{k(U-u)}{a}\right]^{1/k}\right\} \tag{2.3}$$

where $F_U(U)$ is a distribution in a defined period. k is shape factor, a is scale factor and u is location parameter. When $k<0$, the density function is known as the Type II extreme value distribution and when $k>0$, it becomes a Type III extreme value distribution (Weibull distribution). As k tends to 0, equation (2.2) is the Type I extreme value distribution (Gumbel distribution).

In Europe, storms are normally caused by frontal depressions, usually passing in an easterly direction. When one storm mechanism generates the high winds above a site, the Weibull distribution normally gives a good statistical representation of these extreme winds and the probability density function can be written as:

$$f_U(U) = \frac{kU^{k-1}}{c^k}\exp\left[-\left(\frac{U}{c}\right)^k\right] \tag{2.4}$$

The Weibull parameters of k and c for each places are shown in the European Wind Atlas[2.2]. The distribution function is calculated with the following equation:

$$F_U(U) = 1-\exp\left[-\left(\frac{U}{c}\right)^k\right] \tag{2.5}$$

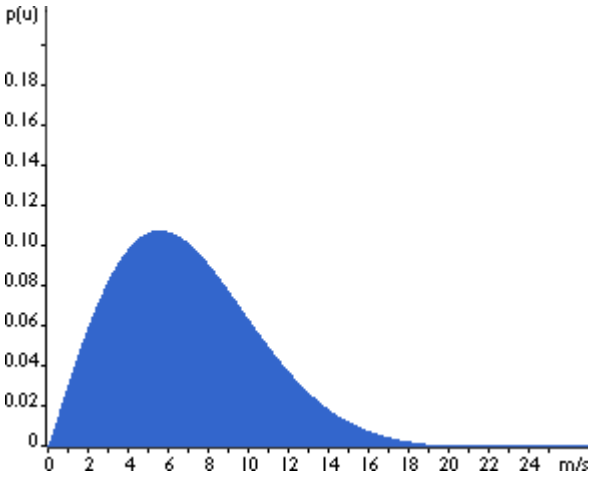

Fig. 2.6 Probability density function of wind velocity

2.1.4 Reference Wind Velocity in Eurocode

The statistical analysis is used to establish the design wind velocity in the construction codes. In the Eurocode, reference wind velocity U is defined as the 10-minute mean wind velocity at 10 m above terrain with the roughness length z_0=0.05m and an annual probability of exceedance of 0.02, which corresponds to a return period of 50 years. The reference wind velocity map of Europe in Eurocode is shown in Fig. 2.7.

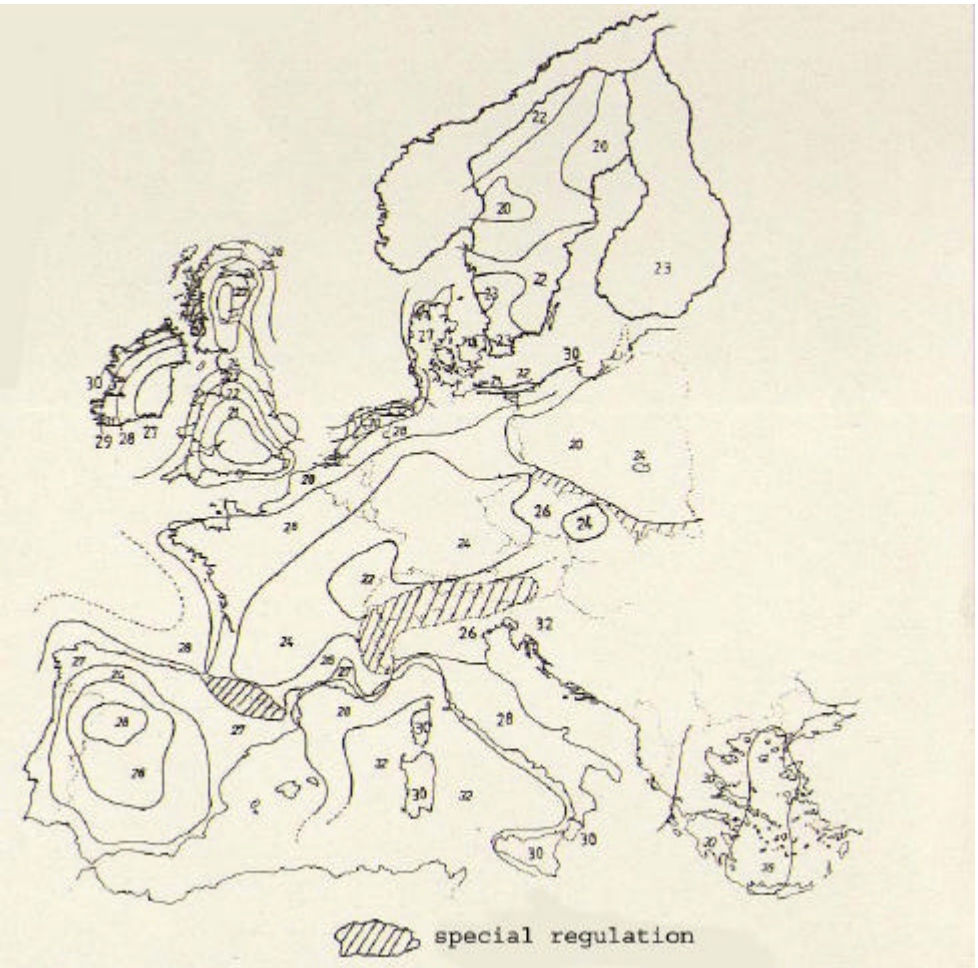

Fig. 2.7 Reference wind velocity map of Europe in Eurocode
Source : Eurocode 1 [2.15]

2.1.5 Turbulence of Wind

Until now wind is described with the mean wind velocity in 10 minutes, but natural wind is always turbulent. Turbulence wind velocity is made of mean wind velocity U and turbulence component $u(t)$. Both are seen in Fig. 2.3. The turbulence component is described below with the standard deviation, time scale and integral length scale.

The standard deviation of fluctuating wind velocity $s_u(z)$ is expressed as:

$$s^2 = \frac{1}{T}\int_{t1}^{t1+T} \left(u(t) - U\right)^2 dt \tag{2.6}$$

where *t1* is the starting time of measurement and T is the data duration. Usually 10 minutes measurement time is used for T value.

The turbulence intensity $I_u(z)$ is defined by using the standard deviation as :

$$I_u(z) = \frac{s_u(z)}{U(z)} \tag{2.7}$$

where $U(z)$ is the mean wind velocity at height z.

The measured turbulence intensities are largely scattered and an universal value is not realistic. In addition generally the intensity is larger in a city than in an open place and it decreases along the height. In order to obtain realistic values some different models have been suggested.

Simiu and Scanlan´s model

Simiu and Scanlan suggest the model of the standard deviation of turbulence wind as follows [2.5]:

$$s^2 = b u_*^2 \tag{2.8}$$

where *ß* is a parameter corresponding to the roughness length, which is shown in the Table 2.1.2. u_* is so called friction velocity that relationship with the mean wind velocity is expressed as:

$$u_* = U(z) \cdot k \Big/ \ln(\frac{z}{z_0}) \tag{2.9}$$

where k is von Karman constant (˜0.4).

Table 2.2 Value of *ß*

z_0 [m]	0.07	0.30	1.0	2.5
ß	6.0	5.25	4.85	4.0

Eurocode

In the Eurocode, the turbulence intensity is directly given by:

$$I_u(z) = \frac{1}{\ln(z/z_0)} \tag{2.10}$$

here z_0 is the roughness length (see 2.1.2).

2.1.6 Power Spectrum of Turbulent Wind

The frequency distribution of turbulent wind direction velocity u is described by the power spectrum. The non-dimensional power spectrum density function $R_N(z, n)$ is defined by using the power spectrum $S_u(z,n)$ as:

$$R_N(z,n) = \frac{nS_u(z,n)}{s_u^2(z)} \tag{2.11}$$

Where as Davenport suggests the non-dimensional power spectrum density $R_N(z,n)$ as:

$$R_N(z,n) = \frac{2}{3}\frac{f_L}{(1+f_L^2)^{3/4}} \tag{2.12}$$

Here f_L is the non-dimensional frequency:

$$f_L = \frac{nL_u^x}{U(z)} \tag{2.13}$$

L_u^x is called integral length scale and assumed with the roughness length. Integral length scale is at heights of 10-240m [2.6] :

$$L_u^x = Cz^m \tag{2.14}$$

where z is the height, C and m depend on the roughness length z_0, which is shown in Fig. 2.8.

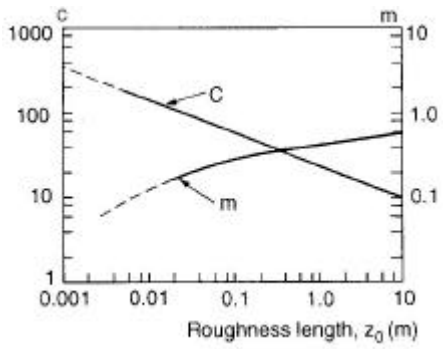

Fig. 2.8 Values of C and m
Source : Dyrbye and Hansen [2.1]

Several other power spectrum density function have been suggested. Fig. 2.9 shows different functions. Von Karman suggested a spectrum in 1948 as follows[2.7]:

$$R_N(z,n) = \frac{4f_L}{(1+70.8f_L^2)^{5/6}} \tag{2.15}$$

In Eurocode 1 the following spectrum form is used:

$$R_N(z,n) = \frac{6.8 f_L}{(1+10.2 f_L{}^2)^{5/3}} \tag{2.16}$$

Harris suggested the next spectrum in 1970[2.1]:

$$R_N(z,n) = \frac{2}{3}\frac{f_L}{(2+ f_L{}^2)^{5/6}} \tag{2.17}$$

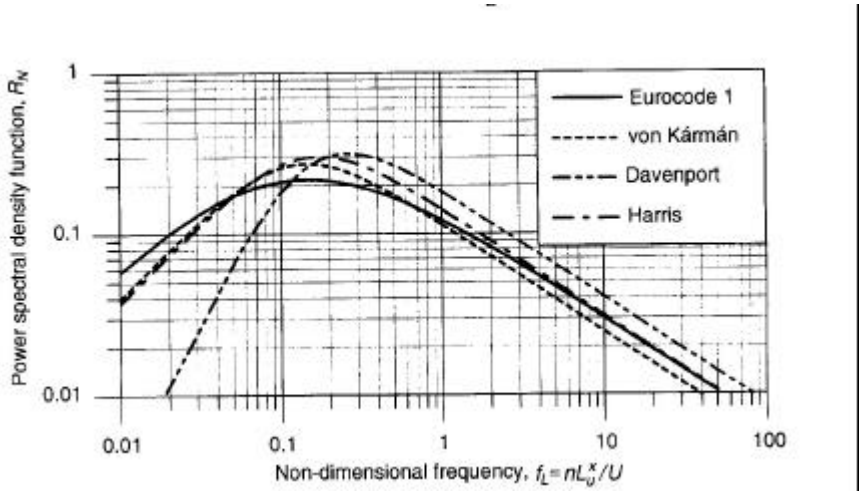

Fig. 2.9 Power spectrum density function for the turbulence component

2.2 Fluid Mechanics

2.2.1 Navier-Stokes Equation and Reynolds number

Wind is a movement of air and air is a fluid. 'Wind force acts on a structure' means that fluid force acts on the structure. Here we discuss the fundamentals of the fluid mechanics, which explain the phenomenon of the air around a structure. Air has a viscosity, that is the reason for most elastic and dynamic problems of the wind. If there was no viscosity in the air, the wind force would not exist. (Fig. 2.10)

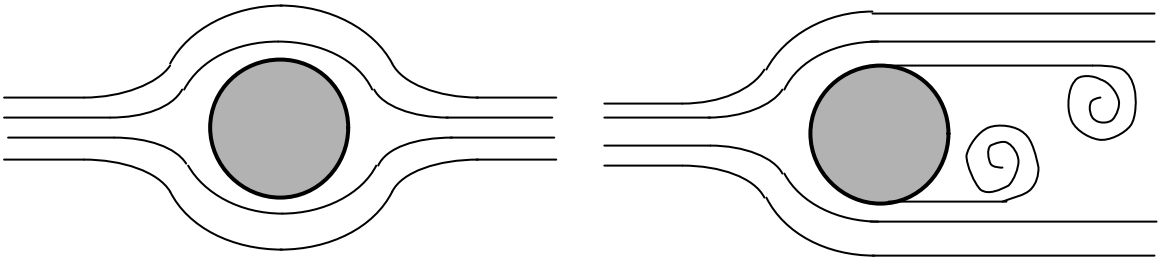

a) ideal fluid b) fluid with viscosity

Fig. 2.10 Aero flow around a column

The equation of motion of the air flow, which takes the effect of the viscosity into account, was developed by Navier in France and Stokes in England in the 19th Century [2.8]. The Navier-Stokes equation is in the orthogonal system as follows:

$$\begin{aligned}
r\left(\frac{\partial u}{\partial t}+u\frac{\partial u}{\partial x}+v\frac{\partial u}{\partial y}+w\frac{\partial u}{\partial z}\right) &= -\frac{\partial p}{\partial x}+m\left(\frac{\partial^2 u}{\partial x^2}+\frac{\partial^2 u}{\partial y^2}+\frac{\partial^2 u}{\partial z^2}\right)\\
r\left(\frac{\partial v}{\partial t}+u\frac{\partial v}{\partial x}+v\frac{\partial v}{\partial y}+w\frac{\partial v}{\partial z}\right) &= -\frac{\partial p}{\partial y}+m\left(\frac{\partial^2 v}{\partial x^2}+\frac{\partial^2 v}{\partial y^2}+\frac{\partial^2 v}{\partial z^2}\right)\\
r\left(\frac{\partial w}{\partial t}+u\frac{\partial w}{\partial x}+v\frac{\partial w}{\partial y}+w\frac{\partial w}{\partial z}\right) &= -\frac{\partial p}{\partial z}+m\left(\frac{\partial^2 w}{\partial x^2}+\frac{\partial^2 w}{\partial y^2}+\frac{\partial^2 w}{\partial z^2}\right)
\end{aligned} \tag{2.18}$$

Here r is the density of air, p is the pressure, u, v and w are fluid velocity of x, y and z directions and here :

$$\frac{\partial u}{\partial x}+\frac{\partial v}{\partial y}+w\frac{\partial w}{\partial z}=0 \tag{2.19}$$

Reynolds number is defined as the ratio between the inertial force term and the viscous force term in the Navier-Stokes equation. In the equation (2.18) the inertial force part is the first part of the left side of the equation and the viscous force is the second part of the right side of the equation. Both forces are:

$$\text{inertial part}: \ \rho \frac{U^2}{L} \tag{2.20}$$

$$\text{viscous part}: \ \mu \frac{U}{L^2} \tag{2.21}$$

U is the fluid velocity, L is the length of the structure, μ is the viscosity coefficient.

Using these, the Reynolds number is expressed as a ratio of the inertial part and the viscous part :

$$\mathrm{Re} = \rho \frac{U^2}{L} \Big/ \mu \frac{U}{L^2} = U \cdot L \Big/ \frac{\mu}{\rho} = \frac{U \cdot L}{\nu} \tag{2.22}$$

Here ν is the kinematic viscosity.

In the high Reynolds number region, the inertial force is dominating and in the low Reynolds number the viscosity is dominating.

2.2.2 Boundary Layer and Disturbed Flow

When the Reynolds number is small enough, air flows along the surface of the structure like an ideal fluid, which assumed to be incompressible and inviscid (Fig. 2.10 a). But in most cases, because of the effect of the viscosity, airflow around the structure is disturbed.

On the surface of a structure, velocity of air becomes small and there, the viscosity force is relatively larger than the inertial force. Such an area is called the boundary layer[2.9]. In the boundary layer kinetic energy is lost by the effect of viscosity and fluid particles lose the energy to flow toward lee side. Then the fluid particles flow back and air can not flow along the surface of the structure any more.

The phenomenon is called a separation of flow. In the separated flow, the velocity is changeable and it gives unstable air-force to the structure. The separated flow is grown and the high frequency vortex is produced. Almost all instability aero dynamic problems are caused by this instability airflow of the boundary layer.

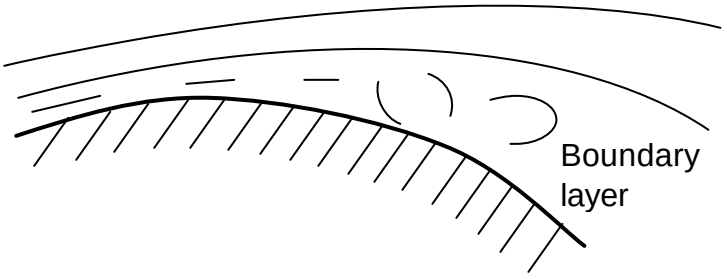

Fig. 2.11 Separation of the flow on the surface of structure

The viscous forces have many effects on the air flow. The vortex structure varies with Reynolds number.

(1) Re˜20 Laminar flow with two vortices
There are two stationary vortices, and the separation points are in front of the column´s surface.

(2) 30 < Re < 5000 Karman vortex street
As Re increases the vortices detach themselves from the column´s surface and form a vortex street behind the column.

(3) 5000 < Re < 2×10^5 Turbulent flow with an agitated boundary layer
As fluid velocity continues to increase, the vortex forms a band of chaotic, irregular flow, called the boundary layer, around the sphere. At this point, the vortices twist in all three dimensions and there is still a pattern of new vortices being formed as others break off.

(4) Re > 10^5 Turbulent flow
At a Reynold's number of approximately 10^5, the boundary layer becomes a "turbulent boundary layer" which extends outward from the back of the sphere.

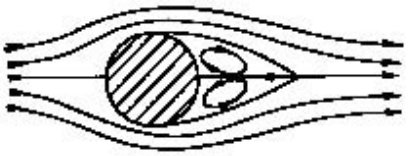

a) Laminar flow with two vortices: Re˜20

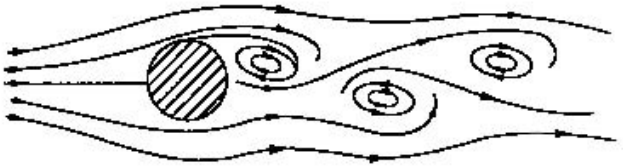

b) Laminar flow with Karman Vortex Streets: 30 < Re < 5000

c) Turbulent flow with an agitated boundary layer: 5000 < Re < 2×10^5

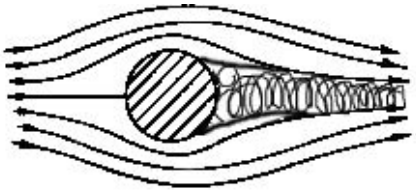

D) Turbulent flow: Re > 10^5

Fig. 2.12 Vortex at different Reynolds numbers
Source : Houghton and Carruters [2.10]

Fluid force which acts on a structure can be explained as the next equation:

$$F = \frac{1}{2} C_D r A v^2 \tag{2.23}$$

Here r is the density of air, A is the area of the wind taking part and v is the velocity of flow. C_D is called drag coefficient, that is changing with the parameter of the shape of the body and the Reynolds number. (Fig. 2.13)

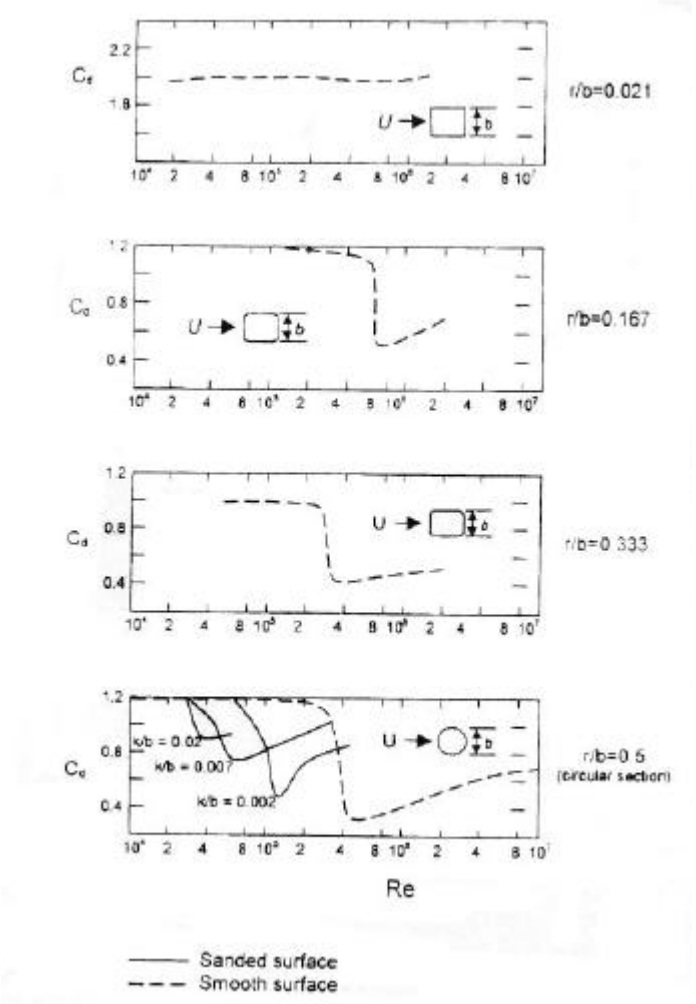

Fig. 2.13 Drag coefficients of bodies at various Reynolds number
Source : Dyrbye and Hansen [2.1]

The conditions of the air flow, such as the separation point, boundary layer, and the vortices, are changing with the form of the body and the Reynolds number [2.5][2.11]. For a slender body along the stream of the air, the boundary layer does not appear and the drag coefficient is close to 0 (Fig. 2.14a). For bluff bodies there is a large wake area in the backward of the body (Fig. 2.14 b, c). Some vortices appear along the edges of a long rectangular structure (Fig. 2.14 d).

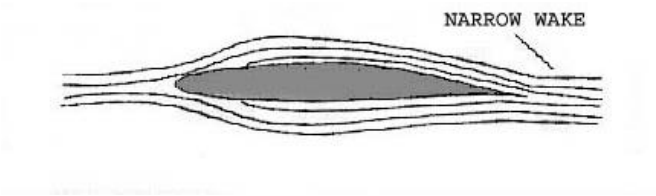

a) slender body along the stream of the air

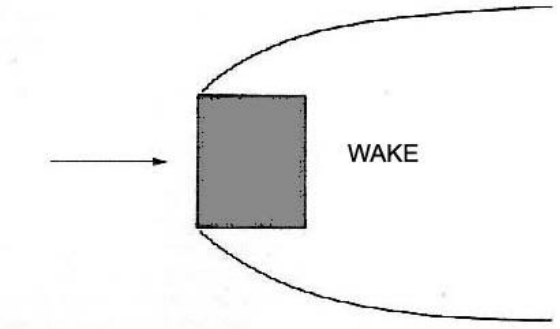

b) bluff body with large wake area behind body

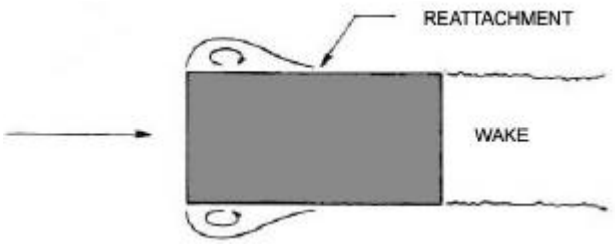

c) bluff body with reattachment

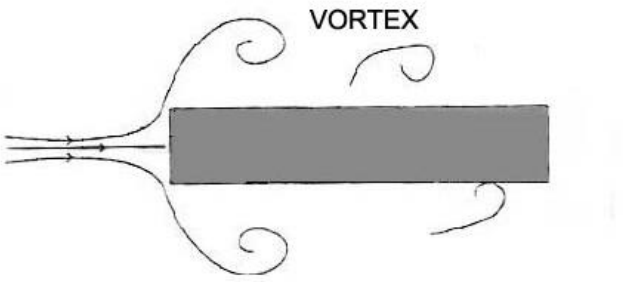

d) long rectangular body with vortices

Fig. 2.14 Air flow around bodies
Source : Simui and Scanlan [2.5]

2.2.3 Aero Elastic Vibration

Vibrations caused by wind and earthquakes are often compared, but from the point of view of the interaction between the structure and the force, there is a large difference between these two phenomena. The vibration induced by an earthquake is a forced vibration, in which the structure is forced from external vibration of the soil. Where as vibration caused by wind involve two types of phenomena : The first one is a forced vibration, in which the structure is emitted by wind. The second one is a self induced vibration, in which the vibration of structure brings an additional aero force which produces a new vibration. As a forced vibration, there is the buffeting, in which the vibration is induced by the turbulence of the wind. Here the phenomena of some aero elastic vibration are explained.

earthquake vibration

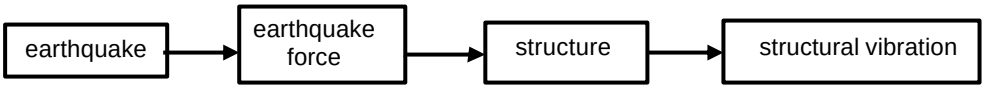

buffeting

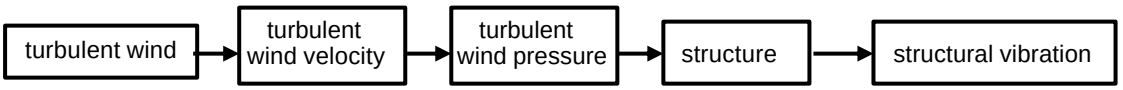

vortex induced vibration, flutter, galloping

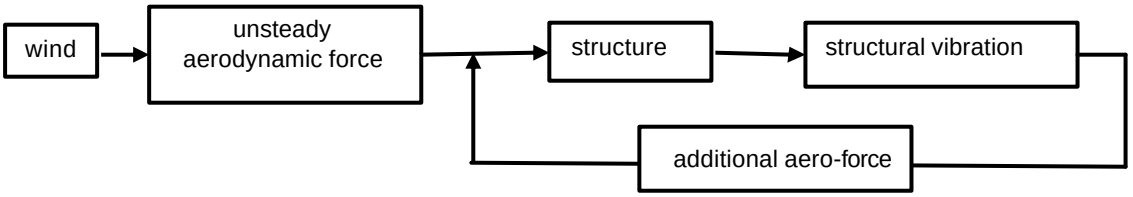

Fig. 2.15 Comparison of structural vibrations under earthquake and wind

Buffeting

Buffeting is a forced vibration, which is induced by turbulence of the wind. The vibration is changing in time and the oscillation of the structure increases proportional to the square of the wind velocity.

Vortex induced vibration

Even though in a constant flow, vortices appear around the structural surface and the vortices induce a vibration of the structure.

Flutter

In flutter, a body starts to vibrate due to any dynamic force like the gust of the wind or vortex. These vibrations disturb the surrounding aero flow and produce an additional aero force. This unsteady aero force increase the vibration of the body furthermore and this phenomenon is called flutter.

2.2.4 Strouhal Number

The frequency f of a vortex is proportional to the wind velocity U and inverse proportional to the diameter of the structure D. Here, the Strouhal number is defined as[2.11]:

$$St = \frac{fD}{U} \tag{2.24}$$

The Strouhal number is dominated by the shape of the body and the Reynolds number. Under a certain wind velocity that produces a vortex the frequency of which is close to the natural frequency of the structure a resonance can happen.

2.2.5 Lock-In Phenomenon

The lock-in phenomenon is usually described as the locking of the frequency of the vortex shedding to the natural frequency of a structure in cross flow[2.12]. For example, it is known that the failure of the Tacoma bridge in 1940 was occurred due to the twist of the deck, which was caused by the vortices(Fig. 2.16) [2.13]. The location of the vortices on the surface of a vibrating rectangular is changing in time. When the number of the vortices on the upper side and the bottom side are different, the heaving motion is brought (Fig. 2.1.10 a). When the same number of vortices are located asymmetry on the upper and bottom side, the pitching motion is observed (Fig. 2.17 b). When the vortices set in point symmetry, twist movement appears.

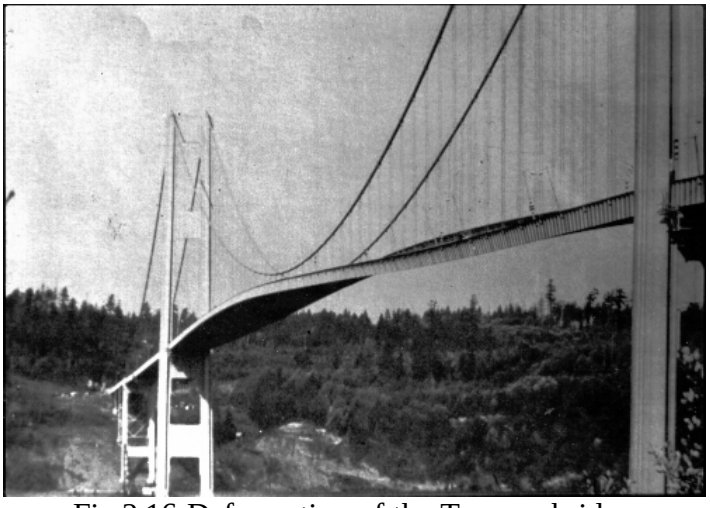

Fig.2.16 Deformation of the Tacoma bridge
Source : Carleton University [2.14]

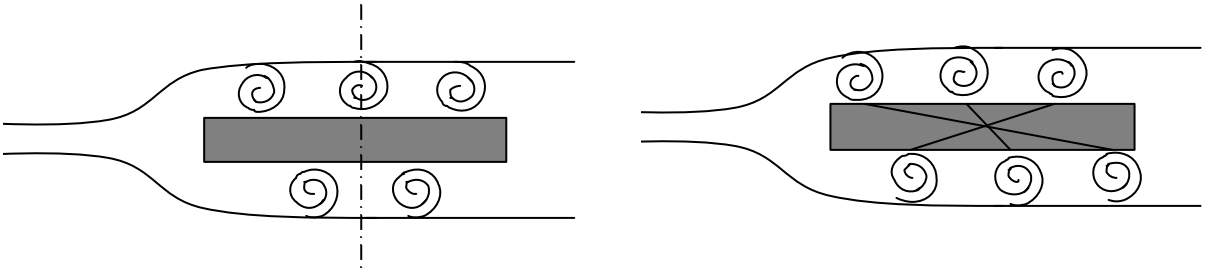

a) heaving motion b) pitching and twist motion

Fig. 2.17 Vortices location on rectangular

2.2.6 Mechanism of Self Induced Vibration

When a body is in a constant aero flow, the dynamic force is caused by the vibration of the body and the frequency of the dynamic load and the vibration of the body are same [2.15]. Here the deformation of the body is :

$$y(t) = y_0 \sin \nu t \tag{2.25}$$

Thus, the velocity is calculated as:

$$\dot{y}(t) = \nu\, y_0 \cos \nu t \tag{2.26}$$

then the dynamic force can be described by using the phase f as:

$$\begin{aligned} f(t) &= f_0 \sin(\nu t + f) \\ &= f_0 \cos f \sin \nu t + f_0 \sin f \cos \nu t \\ &= f_0 \cos f \frac{y}{y_0} + f_0 \sin f \frac{\dot{y}}{\nu\, y_0} \end{aligned} \tag{2.27}$$

The equation of motion is written as follows:

$$m\ddot{y} + c\dot{y} + ky = f(t) \tag{2.28}$$

Here m is mass of the body, c is the mechanical damping, and k is the spring coefficient.
Now we put the equation (2.27) into the equation of motion and put the right part of the equation into the left side. Thus the motion equation can be described:

$$m\ddot{y} + \left(c - \frac{f_0 \sin f}{\nu\, y_0} \right) \dot{y} + \left(k - \frac{f_0 \cos f}{y_0} \right) y = 0 \tag{2.29}$$

When the damping of the second part of the equation is positive, the vibration is reduced. But when the part is negative, the sitting body starts to vibrate and in this situation a self induced vibration appears. Accordingly, in the case of :

$$c - \frac{f_0 \sin f}{\nu\, y_0} < 0\,, \tag{2.30}$$

the self induced vibration occurs. If the mechanical damping is zero or very small and $c \tilde{} 0$, the vibration grows up when the phase f is $0° < f < 180°$.

2.3 Wind Load in Construction Codes

Wind load which acts on structure is a dynamic load and the dynamics originates in different reasons such as turbulence of the natural wind (see 2.1.5), turbulent flow in boundary layer (2.2.2), unsteady aero force by the vibration of structure(2.2.4) and so on. But in some construction codes, dynamic characters are introduced only partly and for the design wind load the dynamic factor is reflected in the dynamic coefficient. In this section the wind load estimation methods of different codes are explained.

2.3.1 Quasi Static Method (DIN 1055 and EC1 2-4)

In DIN 1055 [2.16], first of all, structures are classified according to the dynamic sensitivity of the structure. For the classification, the graph in Fig. 2.18 is used. Only for structures that are sensitive to dynamic loads, the dynamic effect of wind is taken into account.

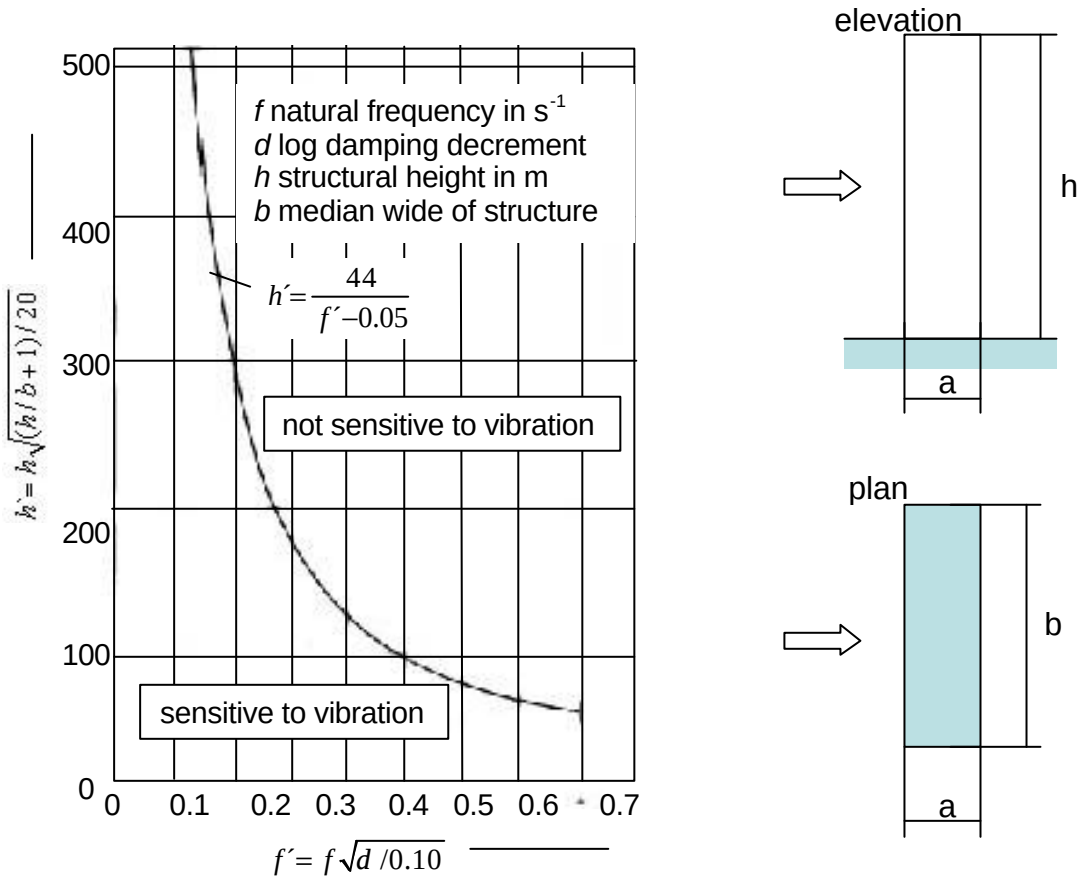

Fig. 2.18 Border of vibration sensitive structure

In Eurocode1 [2.17], the wind force F_w is as the following equation:

$$F_w = q_{ref} \cdot c_e(z_e) \cdot c_d \cdot c_f \cdot A_{ref} \tag{2.31}$$

where c_d is the dynamic coefficient and c_f is the force coefficient, which is obtained by the same theory as the pressure coefficient c_p for a facade element. A_{ref} is the reference area, typically the projected area of the structure that is normal to the wind direction.

In the dynamic coefficient c_d, some dynamic effects of the wind are included as follows.

-Resonance response
-Response due to vortex shedding
-Galloping
-Interference
-Divergence and flutter

The dynamic coefficient is defined as follows:

$$c_d = \frac{1 + 2k_p I_u(z_{ref})\sqrt{k_b + k_r}}{1 + 7I_u(z_{ref})} \tag{2.32}$$

where k_p is the peak factor (see section 3.1). k_b is the background response factor and k_r is the resonance response factor. In the equation (2.32), the dynamic coefficient is defined as the ratio of the dynamic value of the exposure coefficient, which represents the gust load on the structure, to the value of the exposure coefficient, which corresponds to the quasi-static gust load at reference height z_{ref}.
Here the resonance response factor k_r that reflects the aerodynamic admittance function and is defined as:

$$k_r = \frac{p}{d} \cdot R_N \cdot R_h \cdot R_b \tag{2.33}$$

where d is the logarithmic damping of wind direction vibration, R_N is the non dimensional power spectral density function, and R_h, and R_b are vertical and horizontal wind cross-correlation functions.

The power spectral density function R_N expresses the longitudinal turbulence component of natural wind. The cross-correlation factors R_h and R_b transform the spectrum of natural wind to that of wind force for the structure or structural part.

2.3.2 Vortex Excited Vibration (EC1 2-4 Appendix C)

The effect of vortex excited vibrations can be calculated from the inertia force per unit length, F_j, normal to the wind direction at point j of the structure, determined from:

$$F_{i,j} = m_j \cdot (2 \cdot p \cdot n_j)^2 \cdot \Phi_{i,y,j} \cdot \max y_F \tag{2.34}$$

where m_j : the vibrating mass of point j, $n_{i,y}$: natural frequency of crosswind mode i, $\Phi_{i,y,j}$: crosswind mode shape i, max y_F : maximum amplitude of the antinode.

The maximum amplitude of the antinode is defined as

$$\frac{\max y_F}{b} = K_W \cdot K \cdot c_{tat} \cdot \frac{1}{St^2} \cdot \frac{1}{Sc} \tag{2.35}$$

where b : reference width of the cross section at the point of the effective correlation length, K_W : effective correlation length factor, K : mode shape factor, c_{tat} : aerodynamic exciting force coefficient, S_t : Strouhal number, S_c : Scruton number.

2.3.3 Loading Cycle (DIN 4131)

The frequency of the vortex shedding is proportional to the wind velocity. A certain wind velocity raises the critical vortex for the structure. In DIN 4131 [2.18], a construction code for slender antenna mast, the number of the appearance of the wind velocity, which makes critical frequency pressure turbulence, is calculated. It means the fatigue by the high frequency vortex is considered in here. The number of stress cycles N is determined from

$$N = 6.3 \cdot 10^7 T \cdot n_1 e_0 \left(\frac{U_{crit}}{U_0} \right)^2 e^{-\left(U_{crit}/U_0\right)^2} \tag{2.36}$$

where T : lifetime, n_1 : natural frequency of the structure, e_0 : band width factor, U_0 : mean wind velocity defined depends on the zone.
U_{crit} is the critical wind velocity which brings the vortex whose frequency is closed to the natural frequency of the structure. U_{crit} is written as follows:

$$f = St \cdot \frac{U_{crit}}{d} \tag{2.37}$$

where f is the natural frequency of the structure and St is the Strouhal number, shown in 2.2.

2.4 Reference

[2.1] Dyrbye, Claes and Hansen, Svend Ole " Wind Loads on Structures ", Wiley & Sons, 1997

[2.2] Troen, I. and Petersen, E.L., "European Wind Atlas", Riso, National Laboratory, Denmark 1989

[2.3] EUROCODE 1 ENV 1991-2-4, " Base of Design and Actions on Structures, Part 2.4 Wind Actions ",1995

[2.4] Jenkinson, A.F. "the frequency distribution of the annual maximum (or minimum) values of meteorological elements", Quarterly Journal of the Royal Meteorological Society 81, 1955

[2.5] Simui, Emil and Scanlan, Robert H. "Wind Effects on Structures" John Willy & Sons, 1977

[2.6] Counihan, J. "Adiabatic atmospheric boundary layers ", Atmospheric Environment, 1975

[2.7] von Karman, T. "progress in the statistical theory of turbulence", Journal of Material Research 7, 1948

[2.8] Kasahara, E., Shimizu, M. and Maeda, M. "How to Learn Hydrodynamics (in Japanese)", Ohmsha,1986

[2.9] Sachs, Peter "Wind Force in Engineering", Pergamon Press, 1972

[2.10] Houghton, E.L. and Carruthers, N.B. "Wind Forces on Buildings and Structures", Edward Arnold, 1976

[2.11] Bertin, J.J. and Smith M.L., "Aerodynamics for Engineers", Prentice Hall, 1989

[2.12] Dyrbye C. and Hansen, S. O., "Wind Loads on Structures", John Wiley & Sons, 1996

[2.13] Farquharson, E.B. Aerodynamic Stability of Suspension Bridges, a report of an investigation, the structural research laboratory, Washington University, 1950

[2.14] Department of Civil and Environmental Engineering, Carleton University http://www.civeng.carleton.ca/

[2.15] "Structural Design Concepts for Earthquake and Wind", Architectural Institute of Japan 1999 (in Japanese)

[2.16] DIN 1055 Tile4, Lastannahme für Bauten Windlasten, 1986

[2.17] EUROCODE 1 ENV 1991-2-4, " Base of Design and Actions on Structures, Part 2.4 Wind Actions ",1995

[2.18] DIN 4131, " Steel radio towers and masts ", Nov. 1991 (German code)

3 Vibration Analysis of Glass Facades under Wind Load

3.1 Introduction

To estimate the dynamic wind load on a facade element which includes the effect of the motion of the facade itself, numerous simulations were done. Usually for the design of a facade of a building, the quasi-static wind load is used. The estimation of dynamic behaviour is not described in some construction codes. In DIN 1055, there is a description of the dynamic problem for facades[3.1]. :

If the natural frequency of the surface vibration is very low (less than 5Hz), the vibration effect must be considered.

In this section, the motion of facade elements of a building that is located in urban area under turbulent wind is simulated in time series. The simulation is conducted with the finite element program ANSYS©. The facade models are supported in different manners and have different surface areas. Before the time simulations the modal analysis for each model is done and after simulating the time series behavior, confirmation of the existence of the resonance effect is done by the spectrum analysis of the time series results.

3.2 Modal Analysis

3.2.1 Glass Facade Model

Several models of glass facade that is analyzed in this study are described here. The glass material is the same for all models. Area and manner of support are applied as parameters. Concerning support systems, the following two types are used:

Linear support on 4 sides

It is the most orthodox support system. A glass plate is supported along 4 lines. In this model, the elements on the sides are supported in 2 axes at the side nodes. An example of a facade and the model are shown in Fig. 3.1.

Point-support

Glass is bored near to the corners or on the sides and fitted by holders. This system is popular and often used in recent years to create large glass walls [3.2]. In the model, the plate is supported at nodes in 3 axes directions. Often each glass plate is connected by plastic σr silicon, without having structural effect. In the model 4 edges are free. An example and the model are shown in Fig. 3.2.

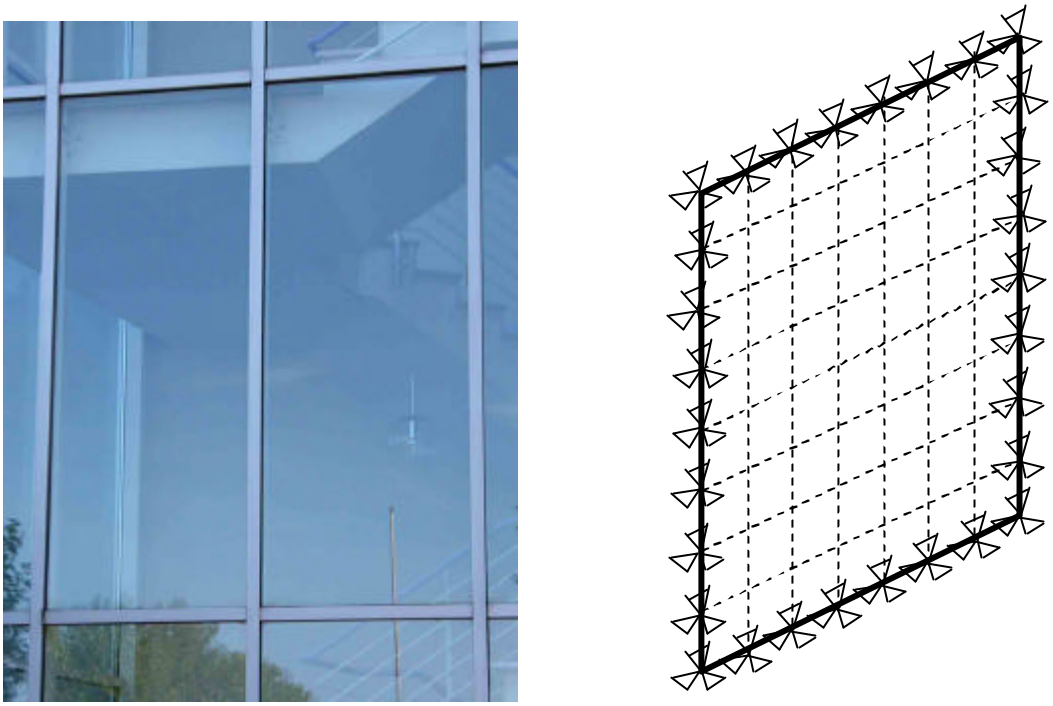

a) b)

Fig.3.1 Linear support on 4 sides a)example of a facade b) model of a glass plate and supports

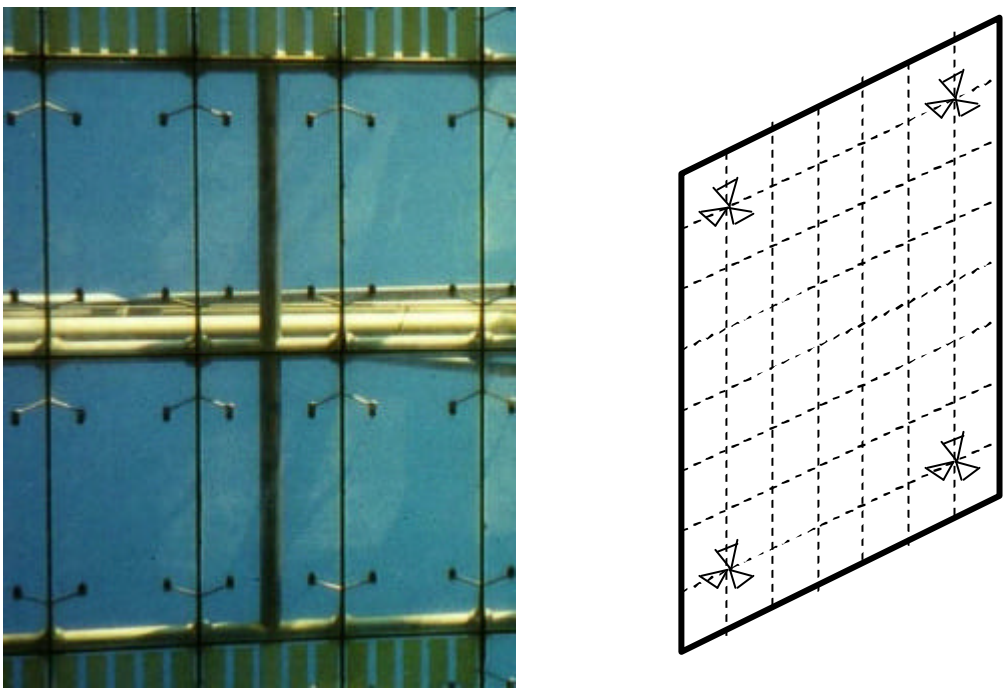

a) b)

Fig.3.2 Point-support a) example of a facade b) model of a glass plate and supports

In Table 3.1, properties of the glass plate used for this simulation are summarised. The different sizes of glass plates are used. The support type and geometry for each plate are shown in Fig. 3.3, 3.4 and 3.5.

Table.3.1 Material characters of the glass

material	ESG, single sheet
stiffness	70000 N/mm^2
density	25kN/m^3

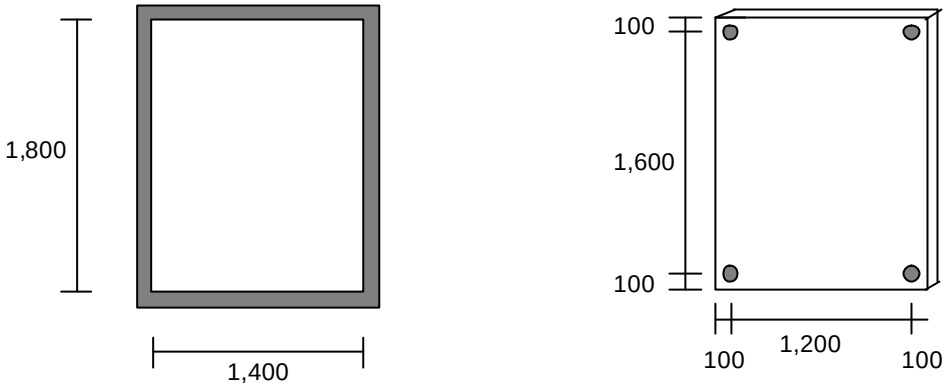

a)linear support on 4 sides b) point-support

Fig. 3.3 Glass plate A 1,400×1,800×8mm

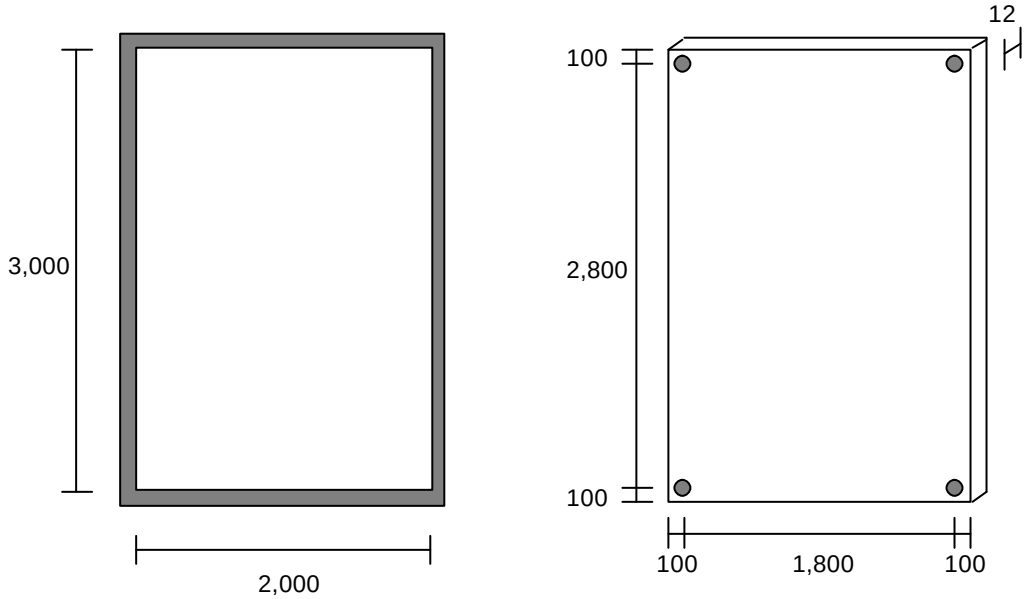

a)linear support on 4 sides b) point-support

Fig. 3.4 Glass plate B 2,000×3,000×12mm

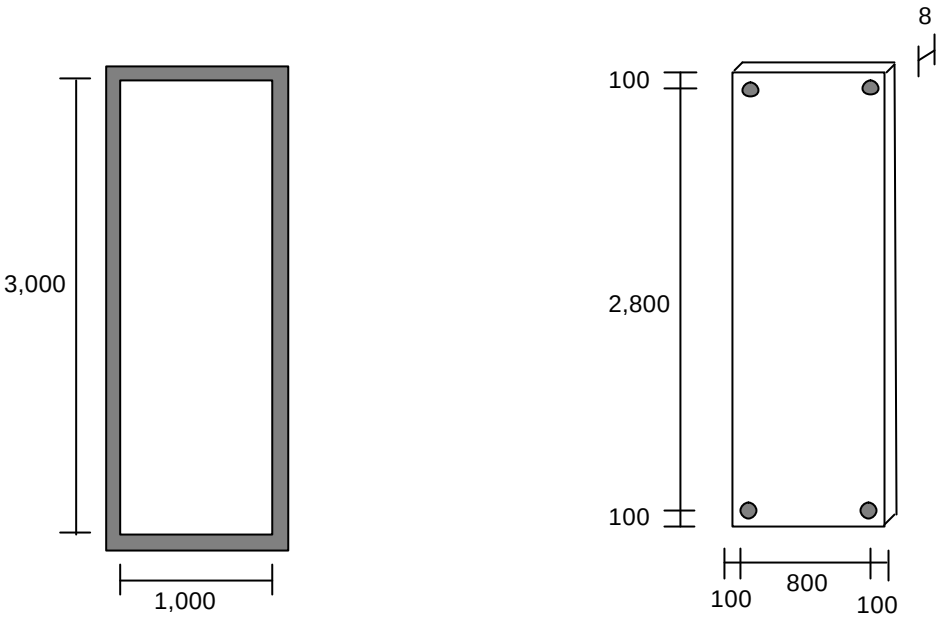

a) linear support on 4 sides b) point-support

Fig. 3.5 Glass plate C 1,000×3,000×8mm

3.2.2 Modal Analysis Results

Modal analyses were carried out for facade models shown in Fig. 3.4-3.6. The natural frequencies of 1st to 3rd modes are given in Table 3.2. The mode shapes for glass plate B and C are shown in Fig. 3.6-3.9. Although the natural frequencies of glass plate A and B are different, mode shapes are similar. Therefore, here only the results of plate B and C are shown.

Table 3.2 Calculation model of facade elements and natural frequencies of them

	natural frequencies (Hz)		
		4 side support	Point support
glass plate A 1,400×1,800×8mm	1st	16.0	7.1
	2nd	34.3	15.1
	3rd	46.1	18.1
glass plate B 2,000×3,000×12mm	1st	10.7	3.6
	2nd	20.5	8.5
	3rd	32.8	11.0
glass plate C 1,000×3,000×8mm	1st	21.8	3.7
	2nd	28.4	14.7
	3rd	39.2	15.5

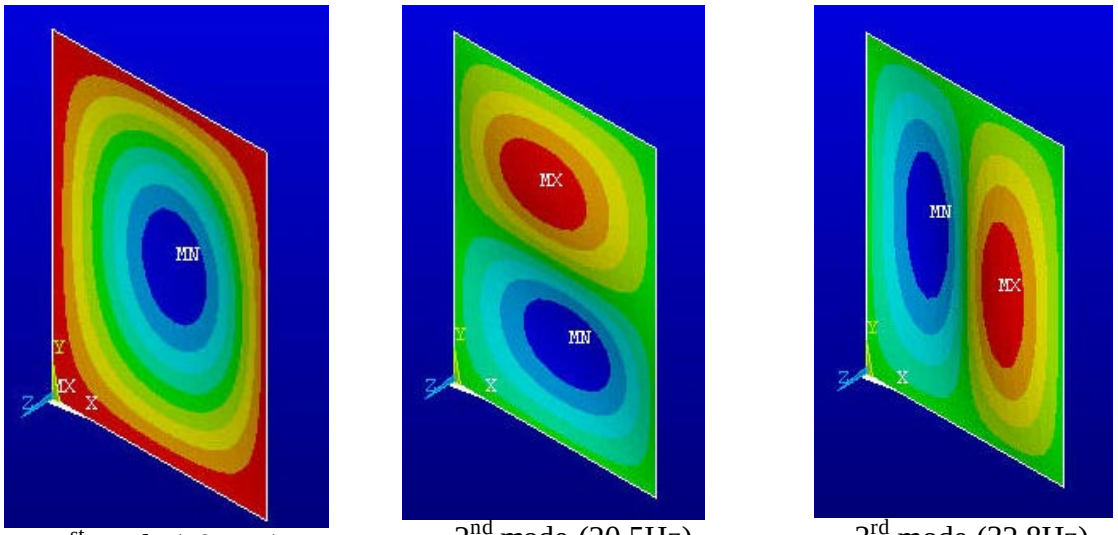

1st mode (10.7Hz) 2nd mode (20.5Hz) 3rd mode (32.8Hz)

Fig. 3.6 Glass plate B linear supported on 4 sides

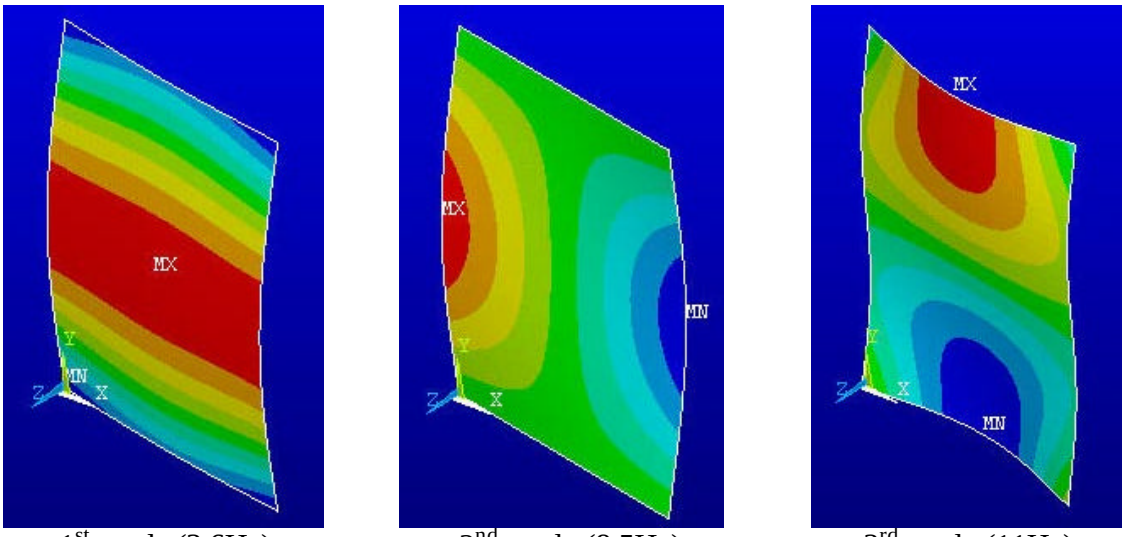

1st mode (3.6Hz) 2nd mode (8.5Hz) 3rd mode (11Hz)

Fig. 3.7 Glass plate B point-support

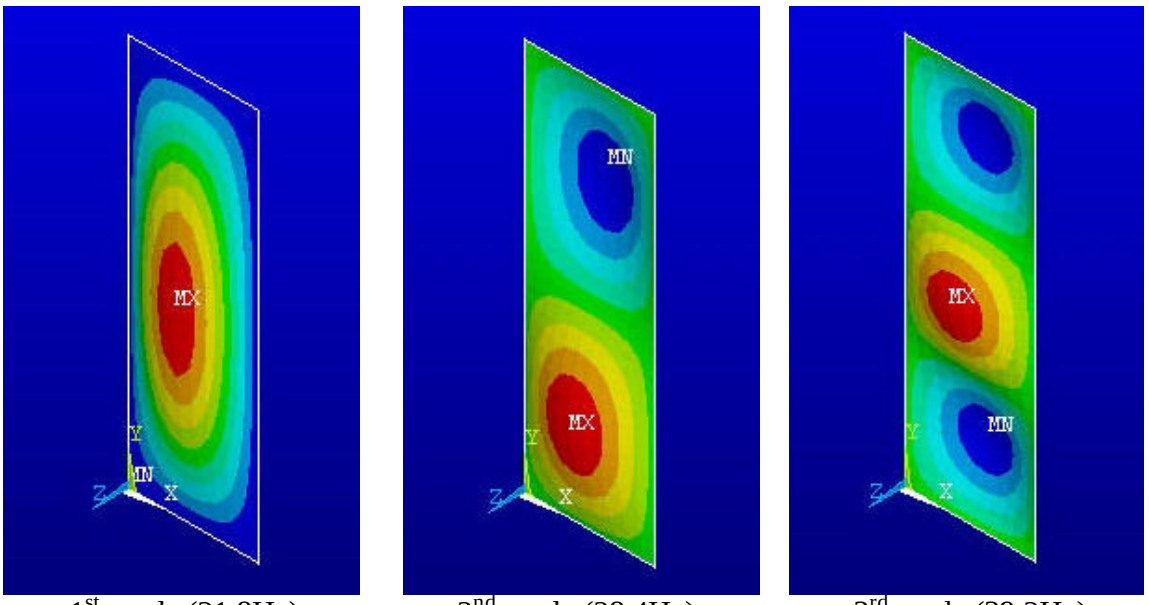

1st mode (21.8Hz) 2nd mode (28.4Hz) 3rd mode (39.2Hz)

Fig. 3.8 Glass plate C linear supported on 4 side

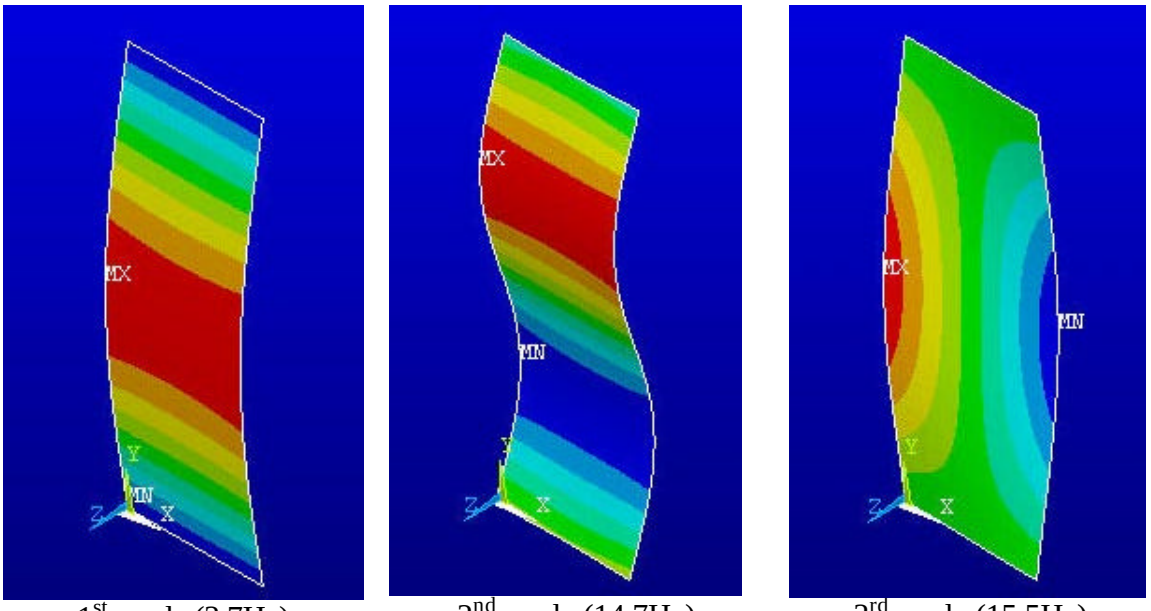

1st mode (3.7Hz) 2nd mode (14.7Hz) 3rd mode (15.5Hz)

Fig. 3.9 Glass plate C point-support

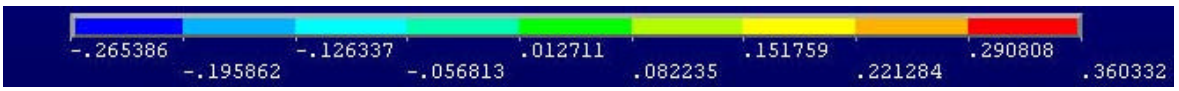

3.3 Time Series Simulation

3.1.1 Equation of Motion

Generally, the equation of motion in the time domain is written as the following equation:

$$m\ddot{X} + D\dot{X} + kX = F(t) \tag{3.1}$$

where m is mass, D is damping, k is stiffness and $F(t)$is wind force.
In this study the external force $F(t)$ is time series fluctuating wind load. The wind load $F(t)$ is proportional to the square of the wind velocity $U(t)$ and written as:

$$F(t) = \frac{1}{2} r c_D U(t)^2 A \tag{3.2}$$

where r is density of air, c_D is drag coefficient and A is area of the wind taking part.
As explained in the chapter 2.1.2, the wind velocity is described with the time averaged part (mean wind velocity) and the fluctuating part. In addition, the relative velocity of wind that acts on a moving body can be expressed as :

$$U_{tot}(t) = U_m + u(t) - \dot{X} \tag{3.3}$$

where $U_{tot}(t)$ is the total wind velocity, U_m is mean wind velocity, $u(t)$ is fluctuating wind velocity and $\dot{X}$ is deformation velocity of moving body.
By applying the equation (3.3), equation (3.2) can be written as follows:

$$\begin{aligned} F(t) &= \frac{1}{2} r A C_D (U_m + u(t) - \dot{X})^2 \\ &\approx \frac{1}{2} r A C_D U_m{}^2 + C_D r A U_m u(t) - C_D r A U_m \dot{X} \end{aligned} \tag{3.4}$$

The first term of the equation which is called static wind load is not dependent on the time. The second term is the time dependent fluctuating term and the third term depends on the motion of the body and is called motion-induced wind load.

By putting this equation of wind load into the equation of motion, (3.1) becomes:

$$m\ddot{X} + D\dot{X} + kX = \frac{1}{2} r A c_D U_m{}^2 + c_D\, r A U_m u(t) - c_D r A U_m \dot{X} \tag{3.5}$$

Furthermore we move the motion induced wind load term from the right side to left side of the equation and reform the equation. Then we get the following equation:

$$m\ddot{X} + \left(D + c_D r A U_m\right)\dot{X} + kX = \frac{1}{2} r A c_D (U_m + u(t))^2 \tag{3.6}$$

For systems with distributed mass, equation (3.6) becomes :

$$[m]\{\ddot{X}\}+([D]+c_D\, r\, AI\{U_m\})\{\dot{X}\}+[k]\{X\}=\frac{1}{2}\, r\, Ac_D I\{U_m+u(t)\}\cdot\{U_m+u(t)\} \qquad (3.7)$$

In this equation the motion-induced wind load includes the damping and the dynamics of wind force that depend on the fluctuation of the natural wind velocity.

3.1.2 Damping

For the time series simulations, the Rayleigh damping is used [3.3]. For the Rayleigh damping, the Rayleigh damping constants a and ß are used. The damping matrix is calculated by using mass matrix [M] and stiffness matrix [K]:

$$[C]=a\,[M]+b\,[K] \qquad (3.8)$$

a [M] and b [K] are called mass-proportional damping and stiffness-proportional damping. The stiffness-proportional damping is mainly caused by inner friction and also called internal viscous damping (Fig. 3.3.1). In many case the structural damping [D] is:

$$[D]=b\,[K] \qquad (3.9)$$

Modal damping ratio for the i^{th} mode x_i is :

$$x_i=\frac{bw_i}{2} \qquad (3.10)$$

where w_i is natural frequency of i^{th} mode.

The damping ratio increases linearly with the natural frequency (Fig. 3.3.2). In this study only the first mode is used. Some studies of the damping of glass facade are being carried out in the Institute of Structural Analysis, Darmstadt University of Technology. We believe that a damping ration of 1% is appropriate for this study.

In terms of the mass-proportional damping, it is also called external viscous damping (Fig. 3.3.1). For the mass-proportional damping the modal damping ratio is given as:

$$x_i=\frac{a}{2w_i} \qquad (3.11)$$

concerning mass-proportional damping, the damping ratio decreases with the natural frequency (Fig. 3.3.2). In the equation of motion (3.7), the damping matrix is the second part

of the equation and $c_D U_m r[A]$ is expressed by applying the mass-proportional damping as follows:

$$a[M] = c_D \cdot U_m \cdot r \cdot [A] \tag{3.12}$$

Then a is

$$a = \frac{c_D \cdot U_m \cdot r \cdot [A]}{[M]} \tag{3.13}$$

If the density of the ESG glass material is 2500 kg/m^3 , the density of air is 1.25 kg/m^3 at 15 ^{0}C, drag coefficient c_D is 1 and a becomes:
$a = 0.005 \cdot U_m$

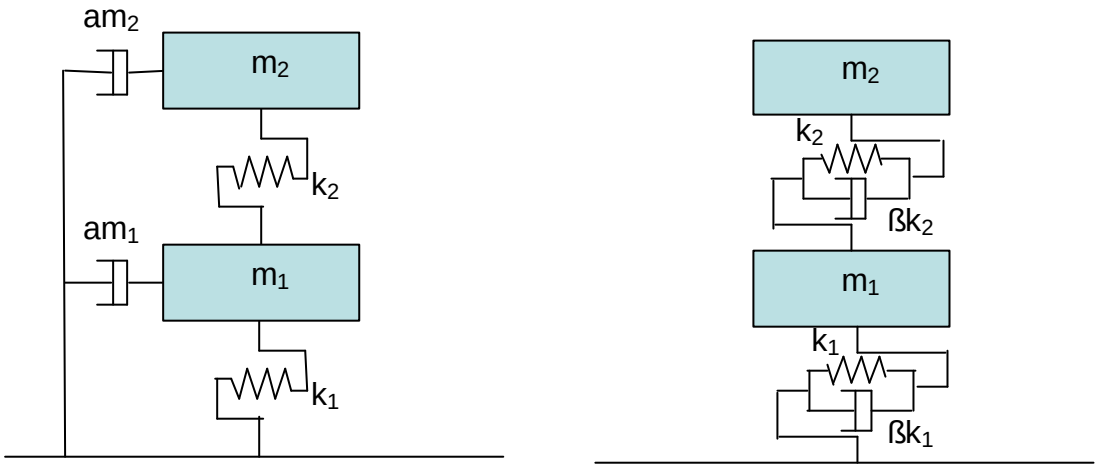

a) b)

Fig. 3.10 Mass-proportional damping a) and stiffness-proportional damping b)

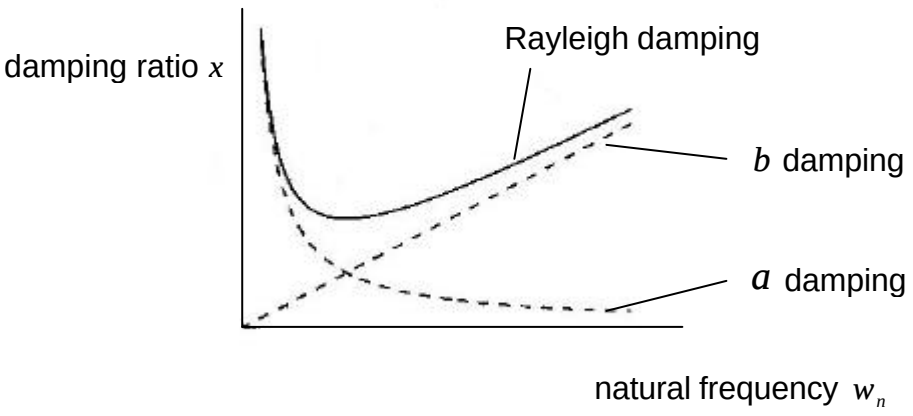

Fig. 3.11 Rayleigh damping

3.1.3 Wind Force

The right side of the equation of motion (3.6) is the fluctuating wind load. Time series wind velocity consists of the mean wind velocity part and fluctuating part.
Mean wind velocity at the height of z is defined by the Davenport model with the equation (2.1). Amplitudes of the wind velocity are calculated by the Fast Fourier inverse transform (Appendix A). The wind velocity in time series can be written as:

$$\begin{aligned} u(t) &= \mathrm{Re}\left[\sum_{m=1}^{M} z_m e^{-iwt}\right] \\ &= \sum_{m=1}^{M} a_m \cos(w_m t + e_m) \\ &= \sum_{m=1}^{M} \sqrt{2 \cdot S(w_m)\Delta w}\cos(w_m t + e_m) \end{aligned} \tag{3.14}$$

where z_m is complex amplitude of 1 to m component wave, a_m is absolute amplitude of 1 to m component wave. e_m is explained as :

$$e_m = 2p P_m \tag{3.15}$$

where P_m is a square distribution between 0 and 1.

The relationship between the Fourier spectrum $F(w)$ and the power spectrum density $S(w)$ is explained by the following equations:

$$S(w) = \frac{2\left|F(w)\right|^2}{\Delta w} \tag{3.16}$$

This equation is deformed as:

$$F(w) = \sqrt{\frac{\Delta w}{2} \cdot S(w)} \tag{3.17}$$

Amplitude a_m is double of the Fourier spectrum (see the section 5.3.1):

$$a_m = 2F(w) \tag{3.18}$$

Then equation (3.1.8) is explained as:

$$a_m = \sqrt{2 \cdot \Delta w \cdot S(w)} \tag{3.19}$$

In this study, the Davenport spectrum (equation (2.12)) is used to calculate the power spectrum density $S(w)$. The standard deviation of turbulence wind is determined by the equation (2.8).

3.1.4 Calculation Results

Time series simulations are carried out for some glass facade models. By solving the equation of motion (3.7) in time series, the time motion of glass facade is solved. The external-force conditions and the calculation conditions are shown in Table 3.3. The calculated models are in Table 3.4.
Mean wind velocity at the height of 20m above ground in an urban area is 30m/s. This value is calculated by using the Davenport model (see the section 2.1.2). The calculation is based on the reference wind velocity 24m/s, which is the wind condition with 50years excepted return period for the south and middle of Germany according to Eurocode.

For the analysis, some of the models that are used for the modal analysis in Section 3.2 are chosen: i.e., glass plate B (2,000×3,000×12mm) with point support and glass plate C(1,000×3,000×8mm) with point support were chosen. These models have the lowest natural frequencies in the facade models, for which the modal analysis was carried out. As an example of linear supported glass, the plate B with 4 line support is selected.

As for the modal analysis, time series simulations are carried out by using the FEM program ANSYS©. Simulation time is 10 minutes, in which the mean wind velocity is considered to be constant.

For all cases, the maximum magnitude of deformation appears at the center of the glass plate. The results of the deformations, deformation velocities and deformation accelerations are observed at the center of the plate.
After analyzing the time series of the motion, the FFT analyses are carried out for all time series results and the spectra of the motions are obtained [3.4]. The results of time series calculations and spectra are shown in Fig. 3.17 to Fig. 3.29.

Table 3.3 External force conditions and calculation conditions

Location of the building	In an urban area in which at least 15% of the surface is covered by building with an average height exceeding 15m, in the middle of Germany
Location of the facade	In the height of 20m above ground, on a wall of the weather side of the building
Mean wind velocity	30m/s
	17m/s
Simulation time	600 s

Table 3.4 Calculation models

Glass area	Support type
Glass plate B 2,000×3,000×12mm	Point support
	4 side support
Glass plate C 1,000×3,000×8mm	Point support

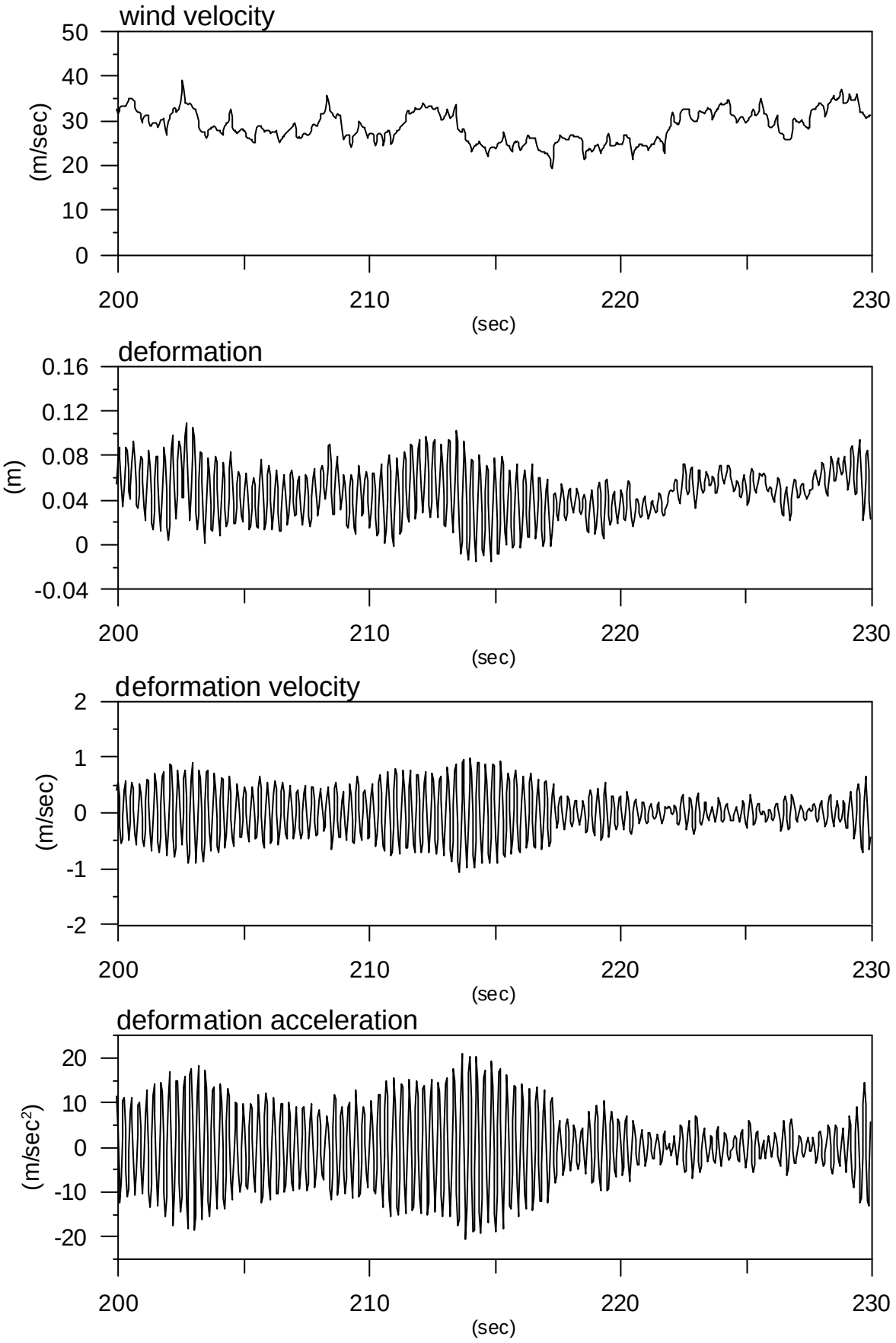

Fig.3.12 Time series of wind velocity, deformation, velocity and acceleration
Glass plate B with point supports under mean wind velocity 30m/s

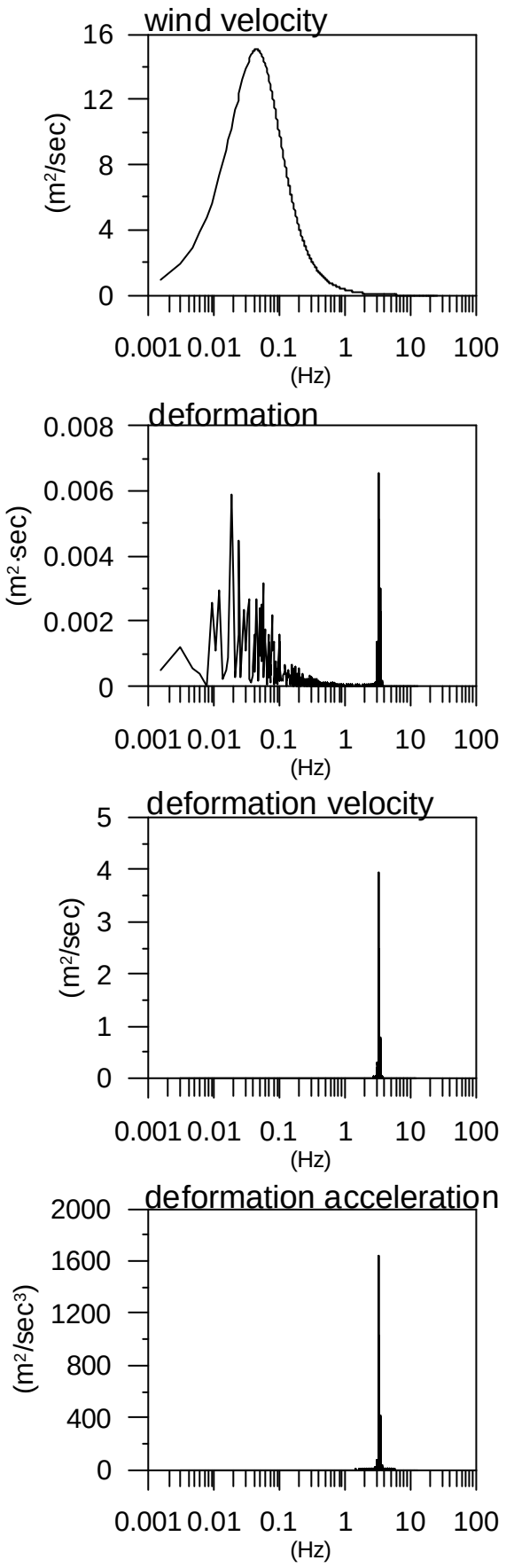

Fig.3.13 Spectrum of wind velocity, deformation, velocity and acceleration
Glass plate B with point supports under mean wind velocity 30m/s

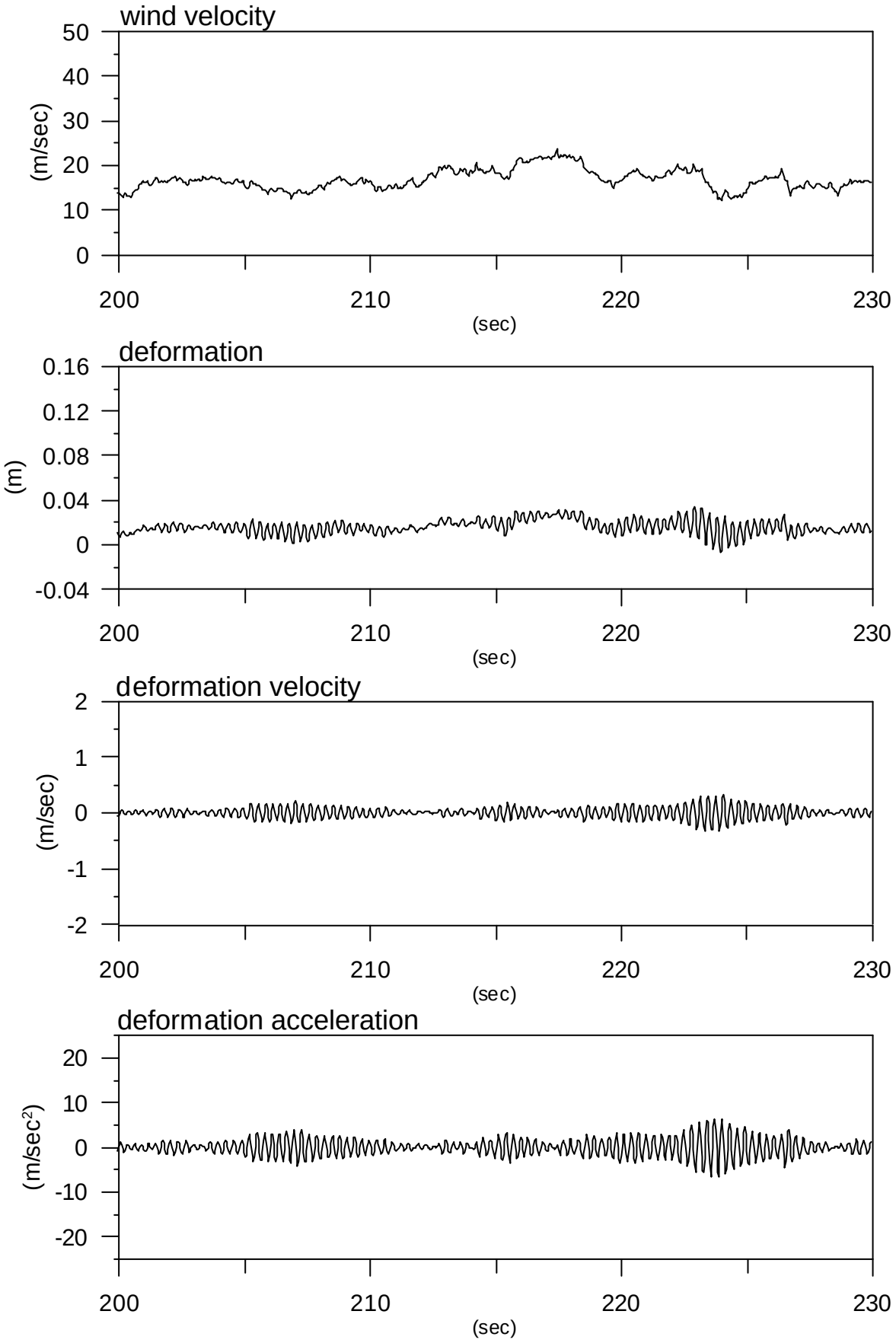

Fig.3.14 Time series of wind velocity, deformation, velocity and acceleration
Glass plate B with point supports under mean wind velocity 17m/s

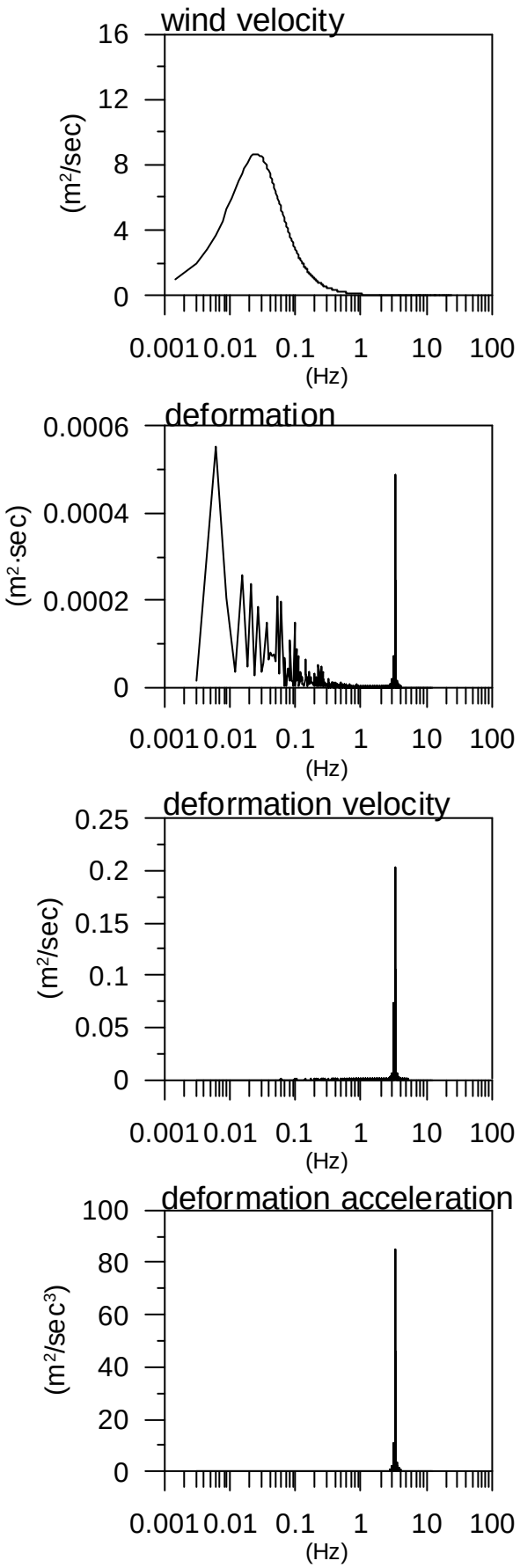

Fig.3.15 Spectrum of wind velocity, deformation, velocity and acceleration
Glass plate B with point supports under mean wind velocity 17m/s

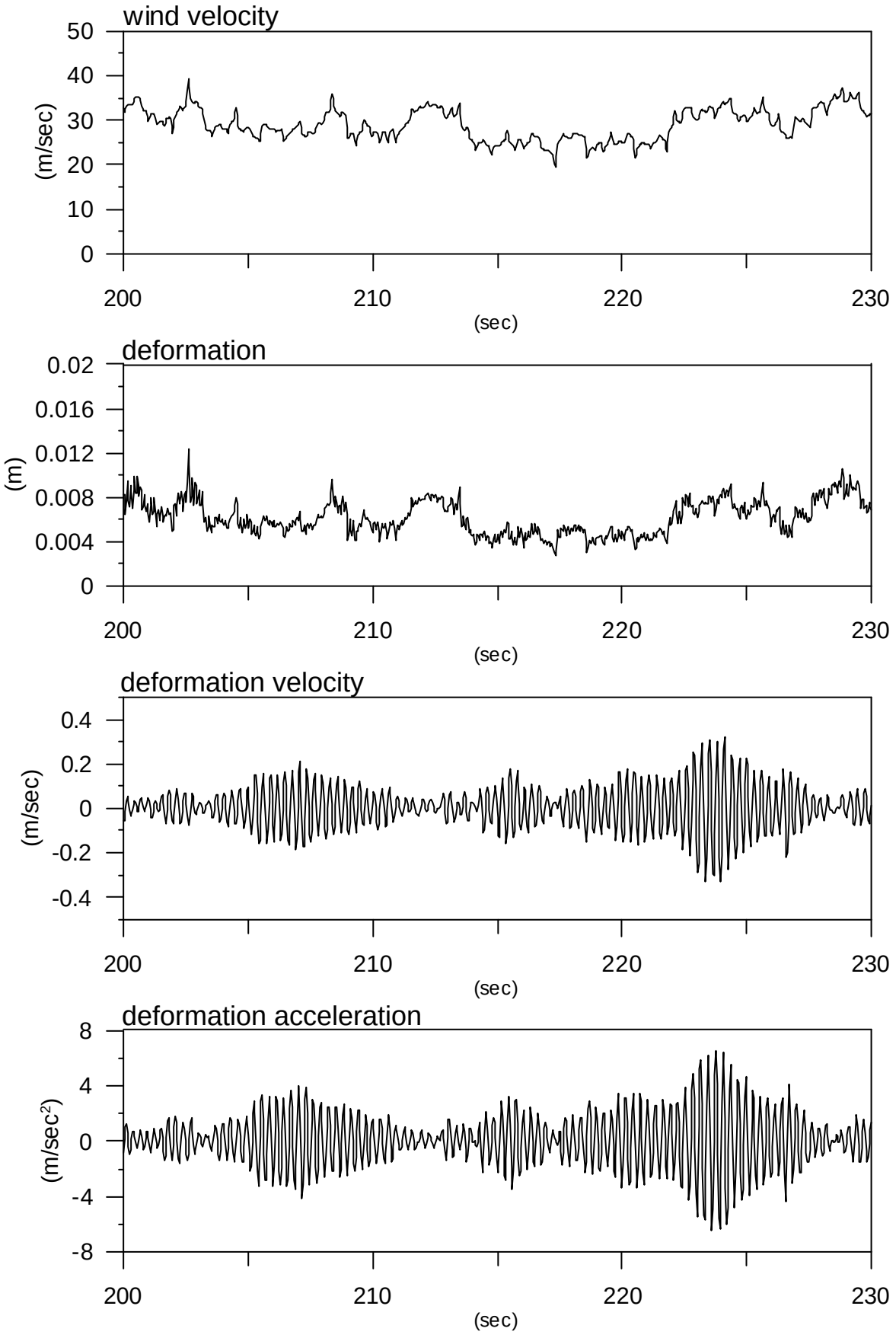

Fig.3.16 Time series of wind velocity, deformation, velocity and acceleration
Glass plate B with 4 line supports under mean wind velocity 30m/s

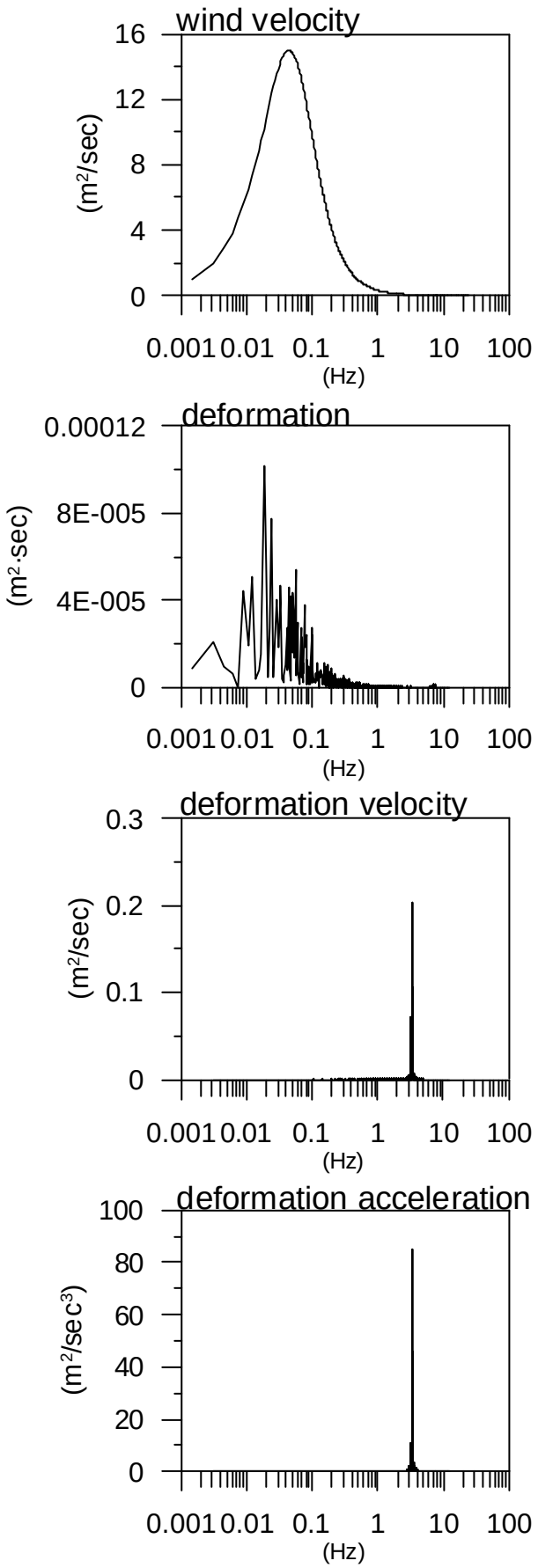

Fig.3.17 Spectrum of wind velocity, deformation, velocity and acceleration
Glass plate B with 4 line supports under mean wind velocity 30m/s

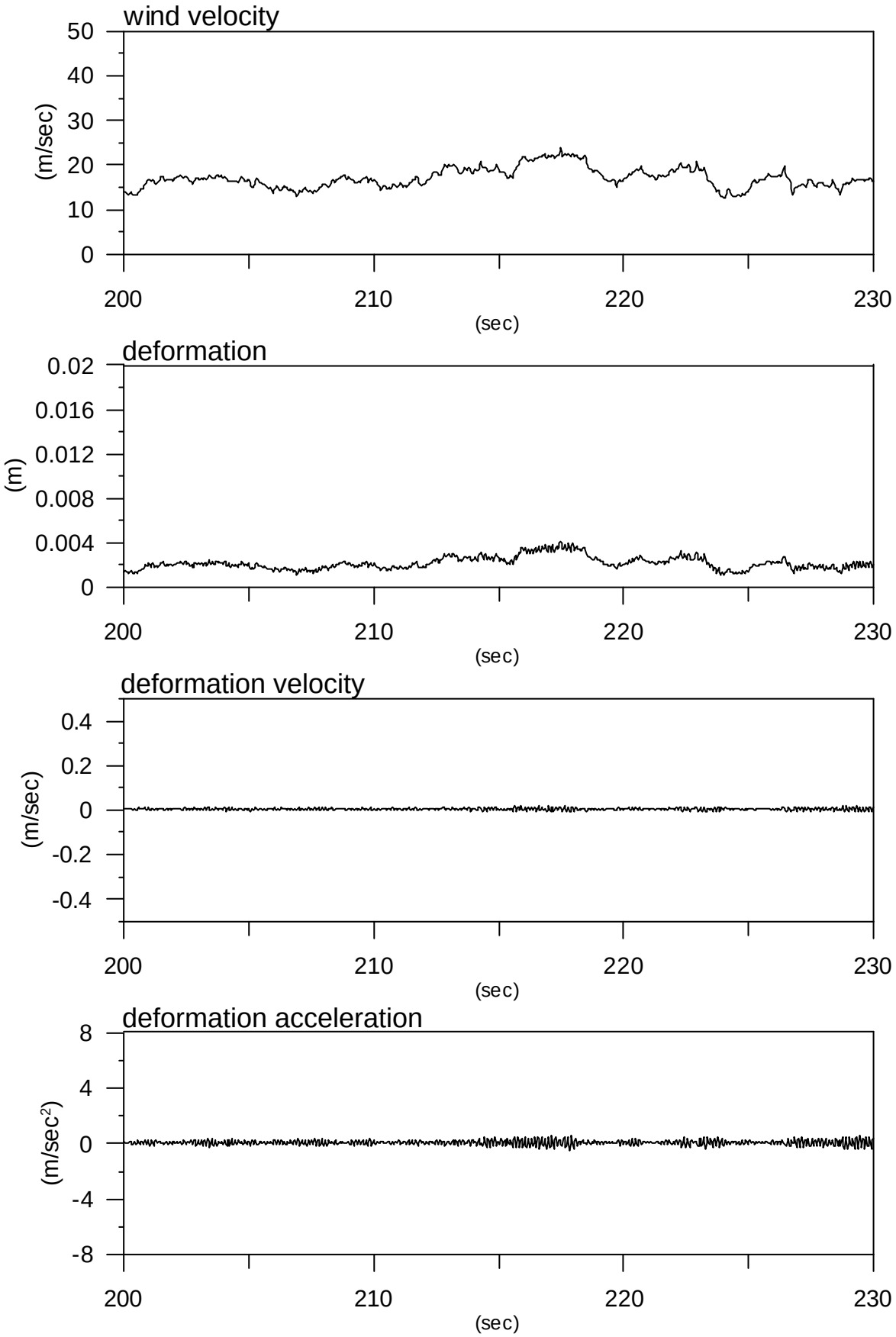

Fig.3.18 Time series of wind velocity, deformation, velocity and acceleration
Glass plate B with 4 line supports under mean wind velocity 17m/s

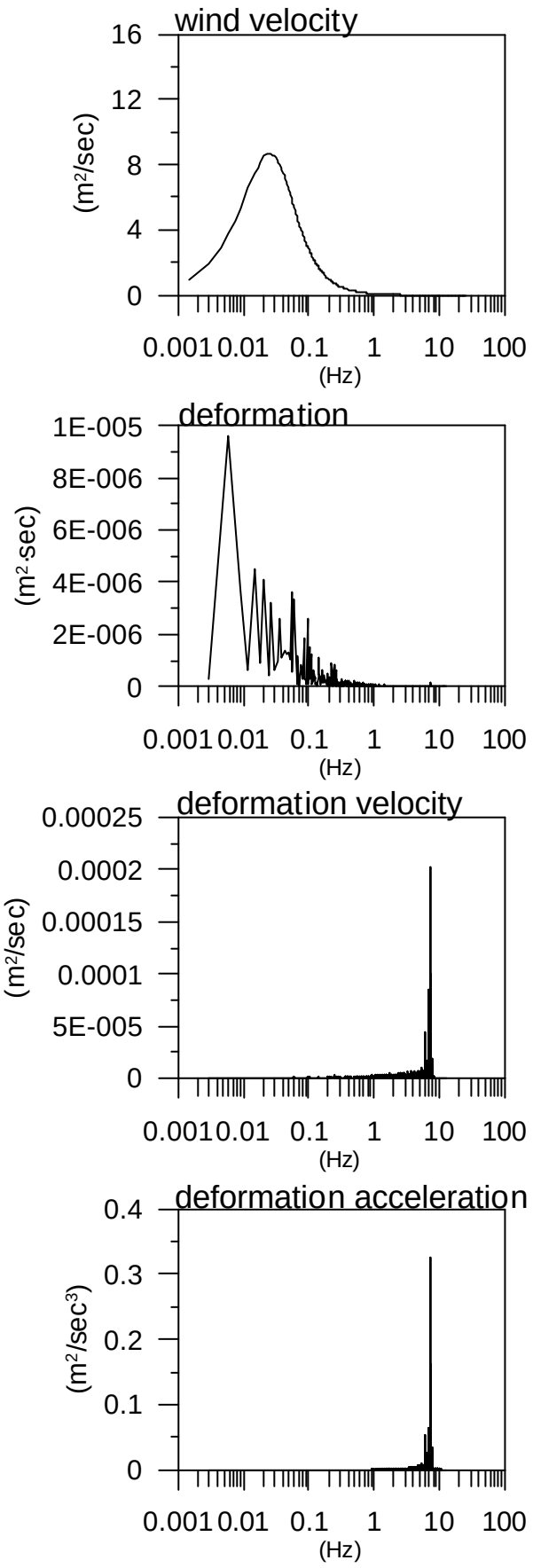

Fig.3.19 Spectrum of wind velocity, deformation, velocity and acceleration
Glass plate B with 4 line supports under mean wind velocity 17m/s

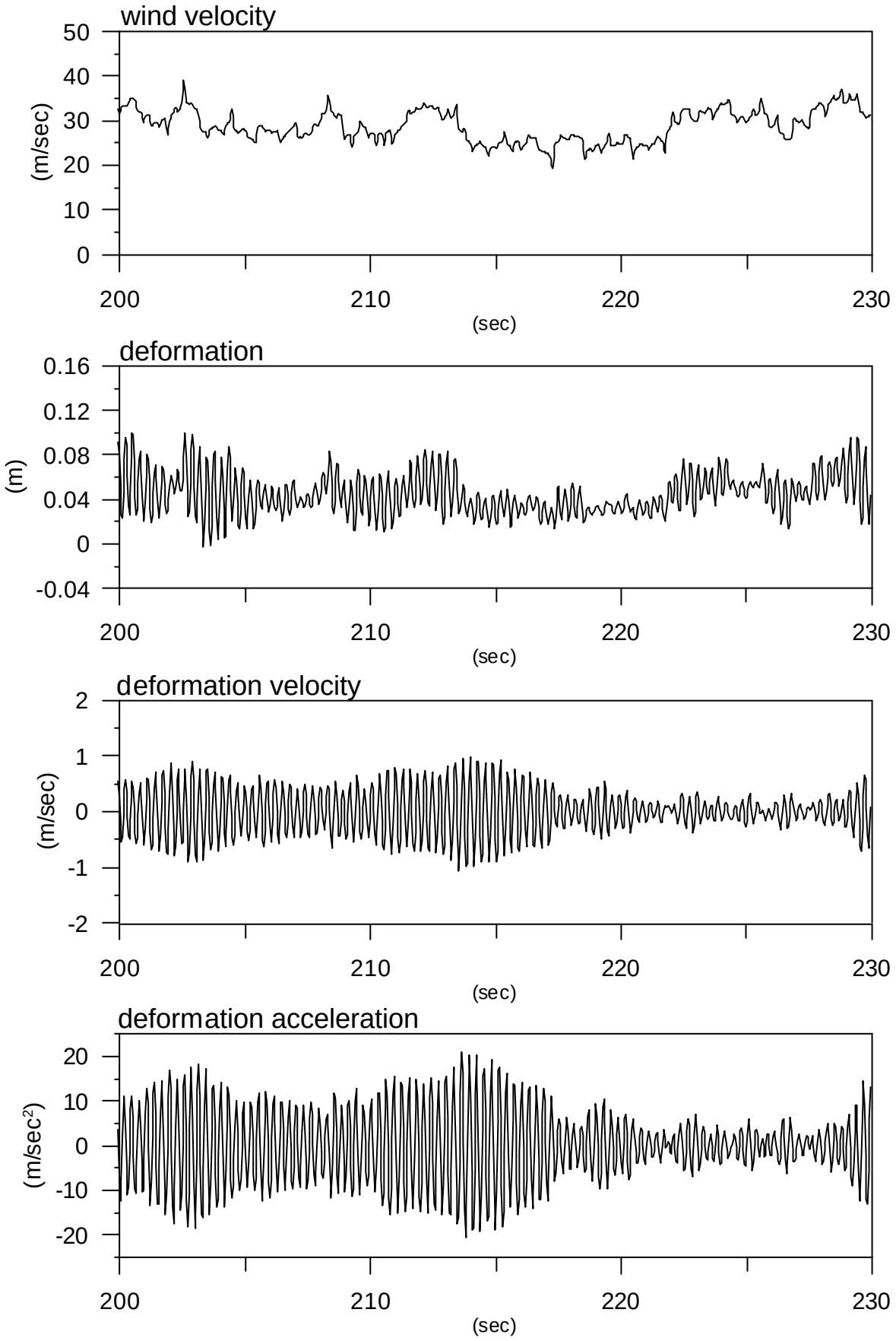

Fig.3.20 Time series of wind velocity, deformation, velocity and acceleration
Glass plate C with point supports under mean wind velocity 30m/s

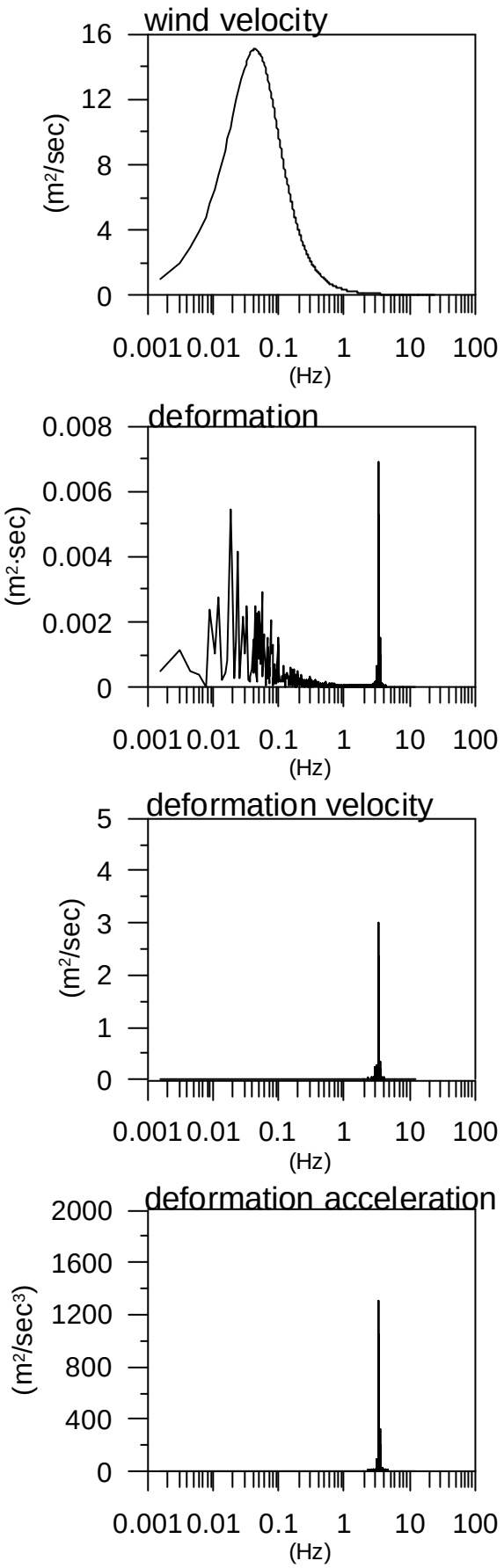

Fig.3.21 Spectrum of wind velocity, deformation, velocity and acceleration
Glass plate C with point supports under mean wind velocity 30m/s

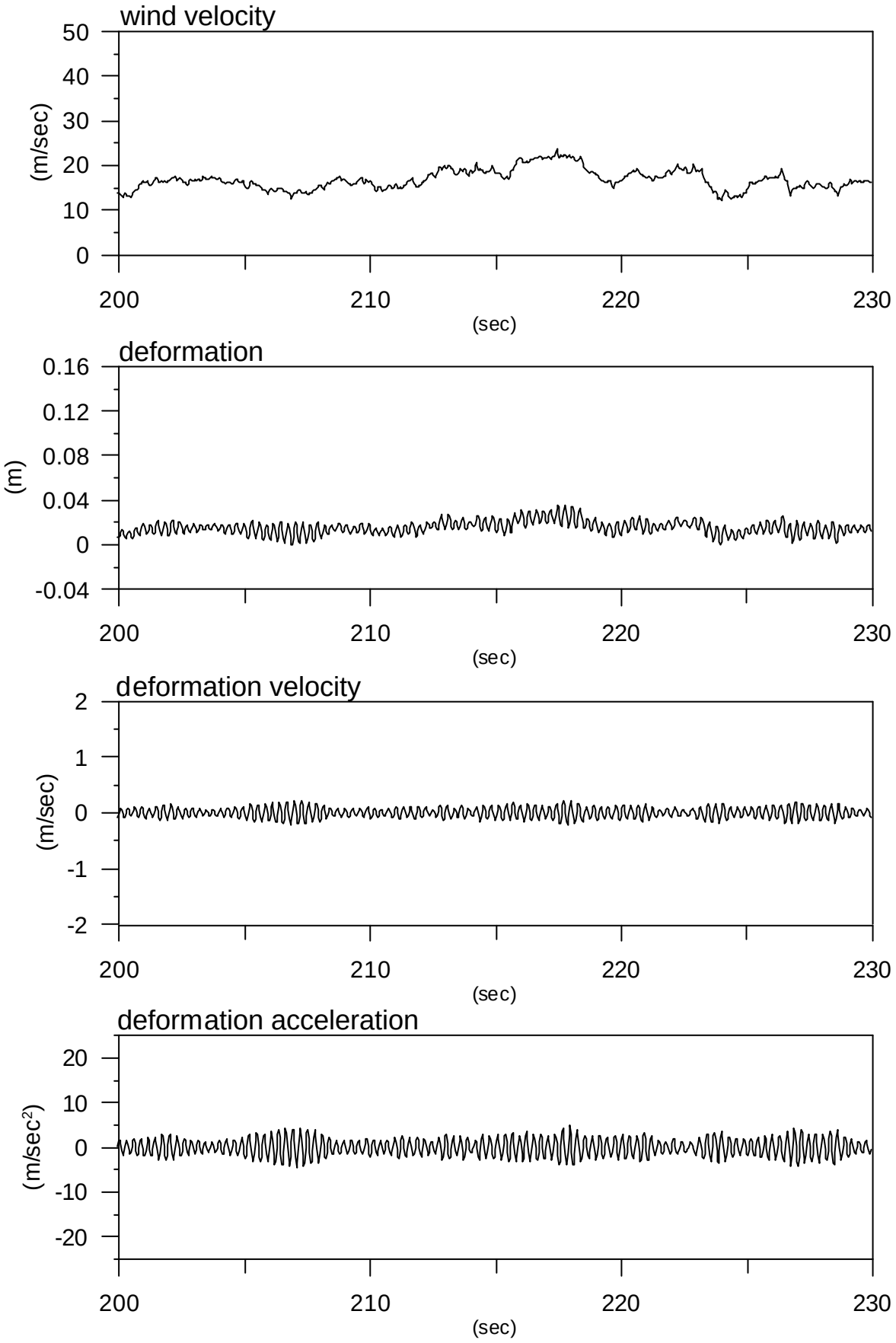

Fig.3.22 Time series of wind velocity, deformation, velocity and acceleration
Glass plate C with point supports under mean wind velocity 17m/s

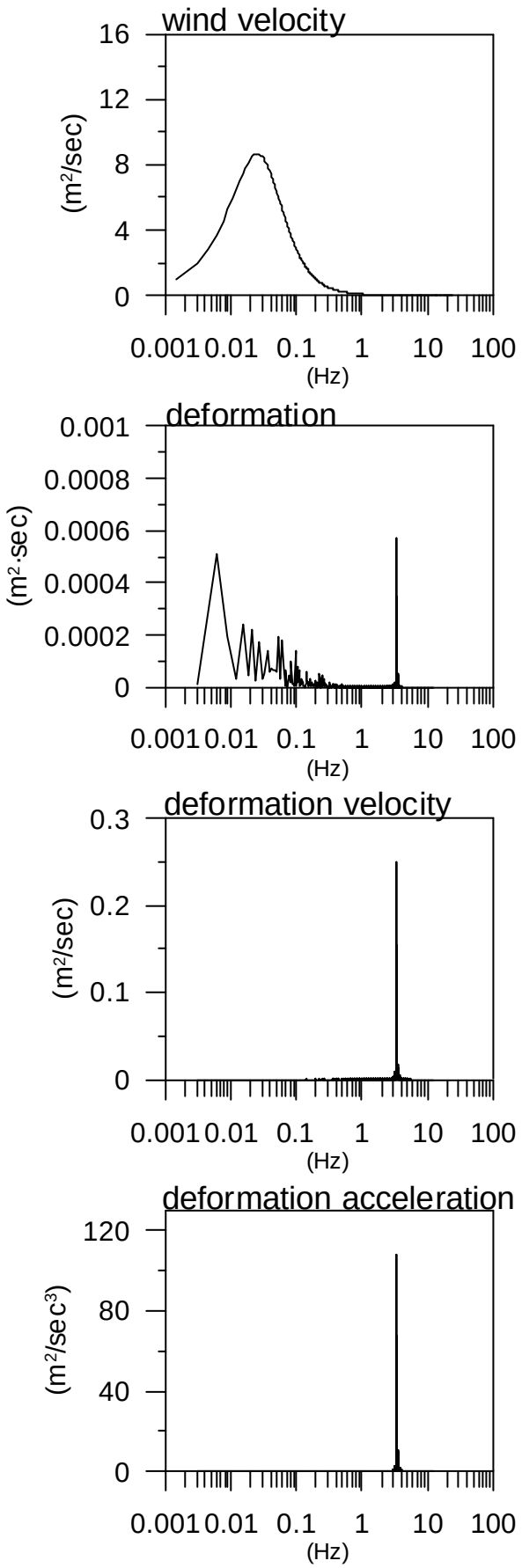

Fig.3.23 Spectrum of wind velocity, deformation, velocity and acceleration
Glass plate C with point supports under mean wind velocity 17m/s

3.3.5 Discussion

The maximum deformations are larger than 10cm in point-support system with plate B and C under the mean wind velocity of 30m/s. The spectra show two peaks. The first one is at the same frequency of the peak of the wind spectrum and the second one is around the first natural frequencies of each facade model. Although the natural frequencies of the glass facades are much larger than the peaks of the spectrum of the wind, in the spectra of response, the peak around the natural frequency is large.
Under the condition of the mean wind velocity of 17m/s, the spectra have the same tendency. However the maximum deformation is around 2cm and much smaller than that of 30m/s mean velocity wind because the wind pressure is proportional to the square of the velocity. The large deformations appear only under extreme winds such as the 50years return period wind.

Concerning the 4 line supported glass, the frequency that closes to the natural frequency of wind turbulence dominates the vibration of the glass. In the time series of the deformation, the wave form looks similar to the wave of fluctuating wind velocity. In the spectrum, the peak is observed at around the natural frequency but is much smaller than the peak at the frequency of the wind. Regarding the magnitude of the deformation, the maximum value is found to be approximately 1.2cm under the condition of the mean wind velocity 30m/s. The value is less than 10% of the deformation observed in the simulation of point-support system with glass plate B and is in the same order of the deformation of point-support system under the condition of the wind velocity of 17m/s (ca. 2cm).

Although the areas of the plates B and C are different, because the first natural frequencies are close, the same tendencies can be seen. On the other hand, the response of the linear support system is significantly different from the point support system, although using the same plate. The motion of glass facades are much more strongly dependent on the support system than on the area of the glass plate.

In terms of deformation velocities and accelerations, the vibration of the first natural frequencies is the dominant factor. In the spectra, the peak around the frequency of the wind is almost not detectable.

As explained in equation 3.5, the motion-induced wind load is dependent on the velocity of the motion of glass. In the next chapter, the motion-induced wind load for glass facades with the large deformation under the extreme wind conditions are discussed by using the results obtained in this chapter.

3.4 Reference

[3.1] DIN 1055 Tile4, “ Lastannahme für Bauten ”, August. 1986 (German code)

[3.2] Wörner J. D., Schneider J. and Fink A. “Glasbau”, Springer, 2001

[3.3] Chopra, A. K., “ Dynamics of Structure”, Prentice Hall, 2001

[3.4] Nussbaumer, H. J., “Fast Fourier Transform and Convolution Algorithms”, Spring-Verlag, 1982

4 Dynamic Wind Load on Glass Facade

4.1 Theory

Here the equation of motion (3.5) is shown again.

$$m\ddot{X} + D\dot{X} + kX = \frac{1}{2}\rho AC_D U_m^{\ 2} + c_D \rho AU_m u(t) - c_D \rho AU_m \dot{X}$$

The first term of the right side of the equation is the static load F_q, which is constant in time. The second term is the fluctuating wind load F_t. It depends on the fluctuating natural wind velocity and it is changing in time. The third term is so called motion induced wind load F_m, which depends on the velocity of the moving structure $\dot{X}$. The second and third terms are the dynamic load. The sum of the fluctuating wind load. The motion induced wind load becomes the dynamic wind load.

In this section, the motion-induced wind loads on glass facades are calculated by using the motions of glass facades, which were determined by time series simulations in Chapter 3.

Time series of motion induced wind load are compared with time series of fluctuating wind load. The spectrum of the motion induced wind load, fluctuating wind load, and the total dynamic wind load are obtained by Fast Fourier Transform.

The first three calculations were carried out on the point-supported glass plate B (details are shown in Fig. 3.5), whose deformation degree and deformation velocity are the largest in Chapter 3. Each calculation is conducted under the condition of the mean wind velocity of 30m/s, 24m/s, and 17m/s.

The time series and spectra are shown in the Fig. 4.1 to 4.6.

As an example of the calculation results on a 4 line supported facade, the dynamic wind load on the 4 line supported glass plate B under a mean wind velocity 30m/s is calculated and the results are shown in the Fig. 4.7. The spectra patterns of the dynamic wind load on the glass plate are shown in the Fig. 4.8.

4.2 Calculation Results

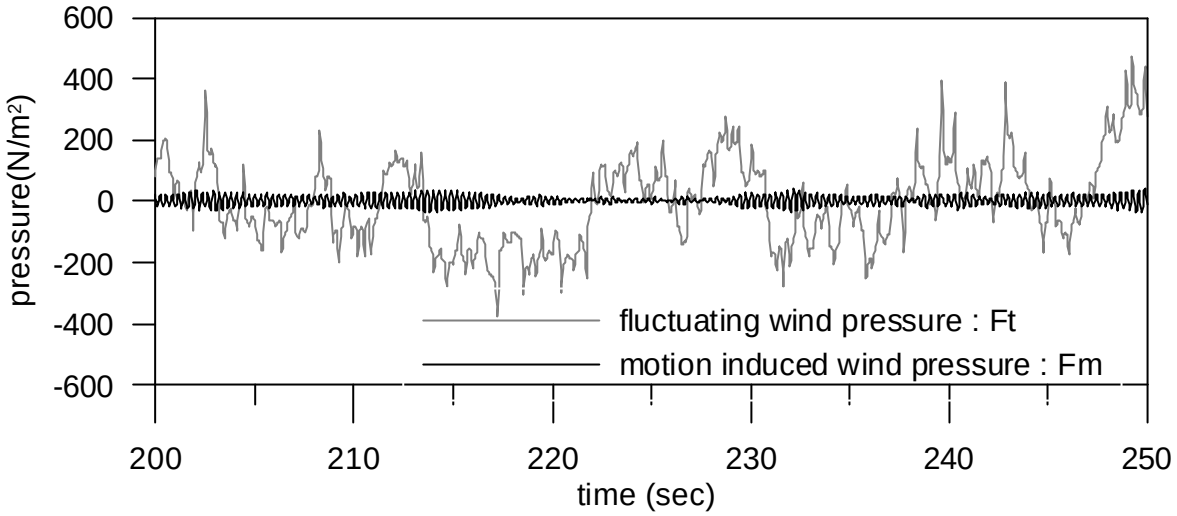

Fig.4.1 Time series of fluctuating wind pressure and motion induced wind pressure
Glass plate B, point support, mean wind velocity 30m/s

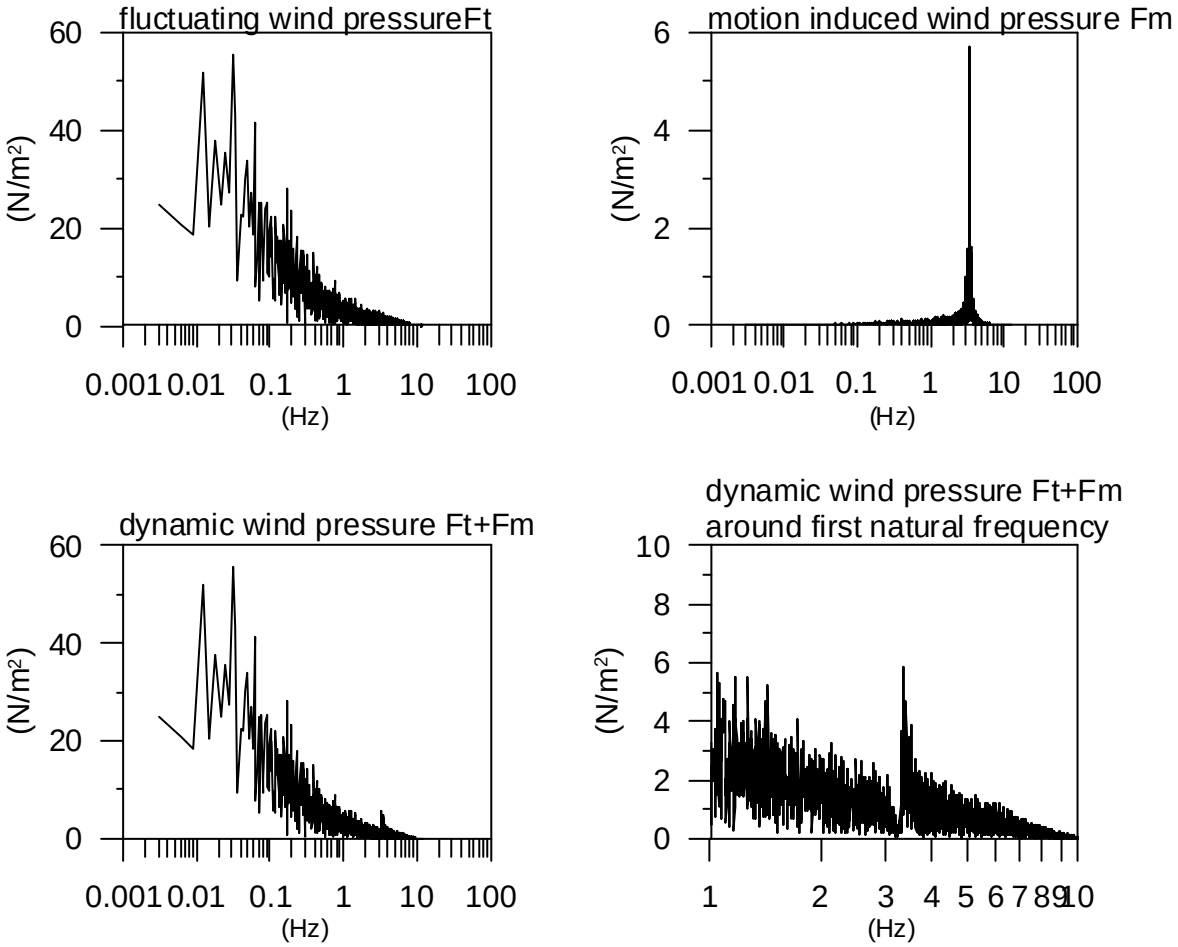

Fig.4.2 Fourier spectrum of fluctuating wind pressure, motion induced wind pressure, dynamic wind pressure (sum of fluctuating wind pressure and motion induced wind pressure) and the extension of the dynamic wind pressures graph
Glass plate B, point-support system, mean wind velocity 30m/s

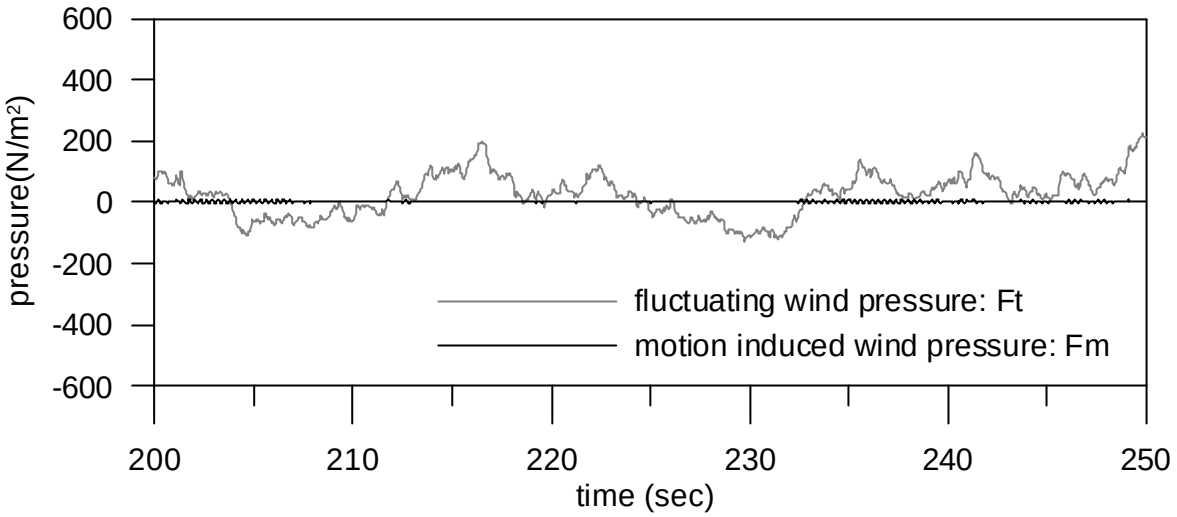

Fig.4.3 Time series of fluctuating wind pressure and motion induced wind pressure
Glass plate B, point support, mean wind velocity 24m/s

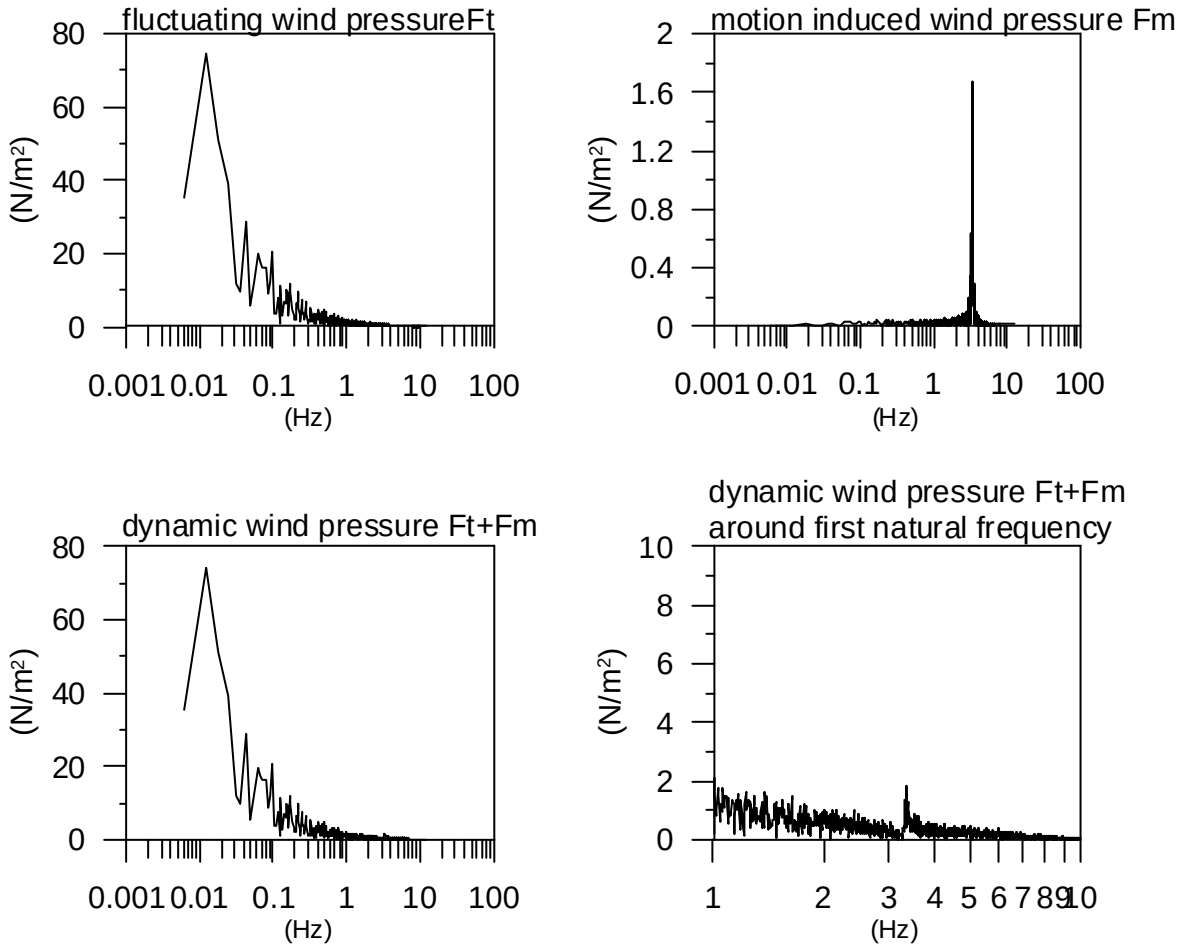

Fig.4.4 Fourier spectrum of fluctuating wind pressure, motion induced wind pressure, dynamic wind pressure (sum of fluctuating wind pressure and motion induced wind pressure) and the extension of the dynamic wind pressures graph
Glass plate B, point-support system, mean wind velocity 24m/s

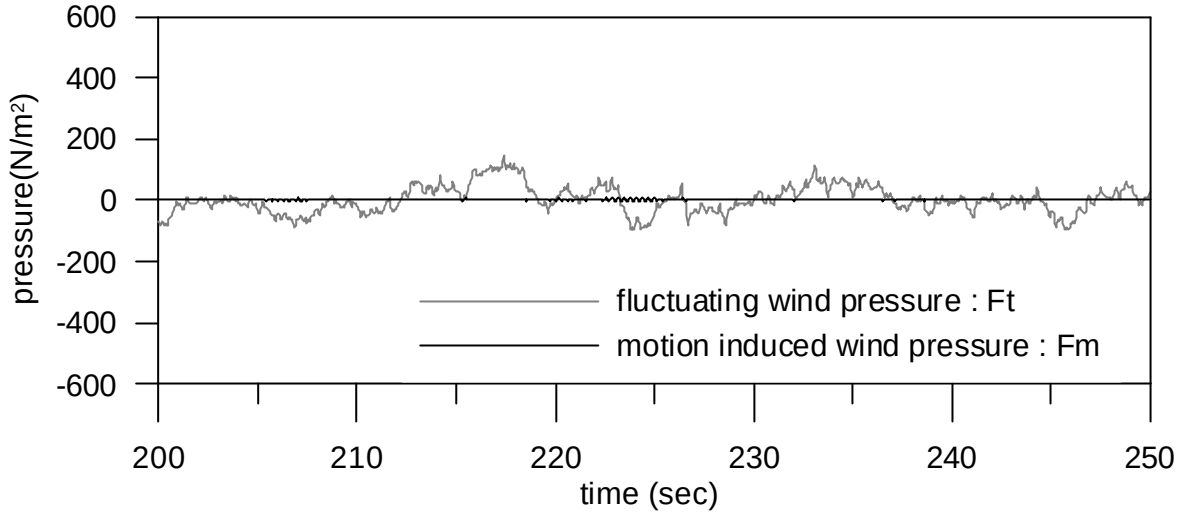

Fig.4.5 Time series of fluctuating wind pressure and motion induced wind pressure
Glass plate B, point support, mean wind velocity 17m/s

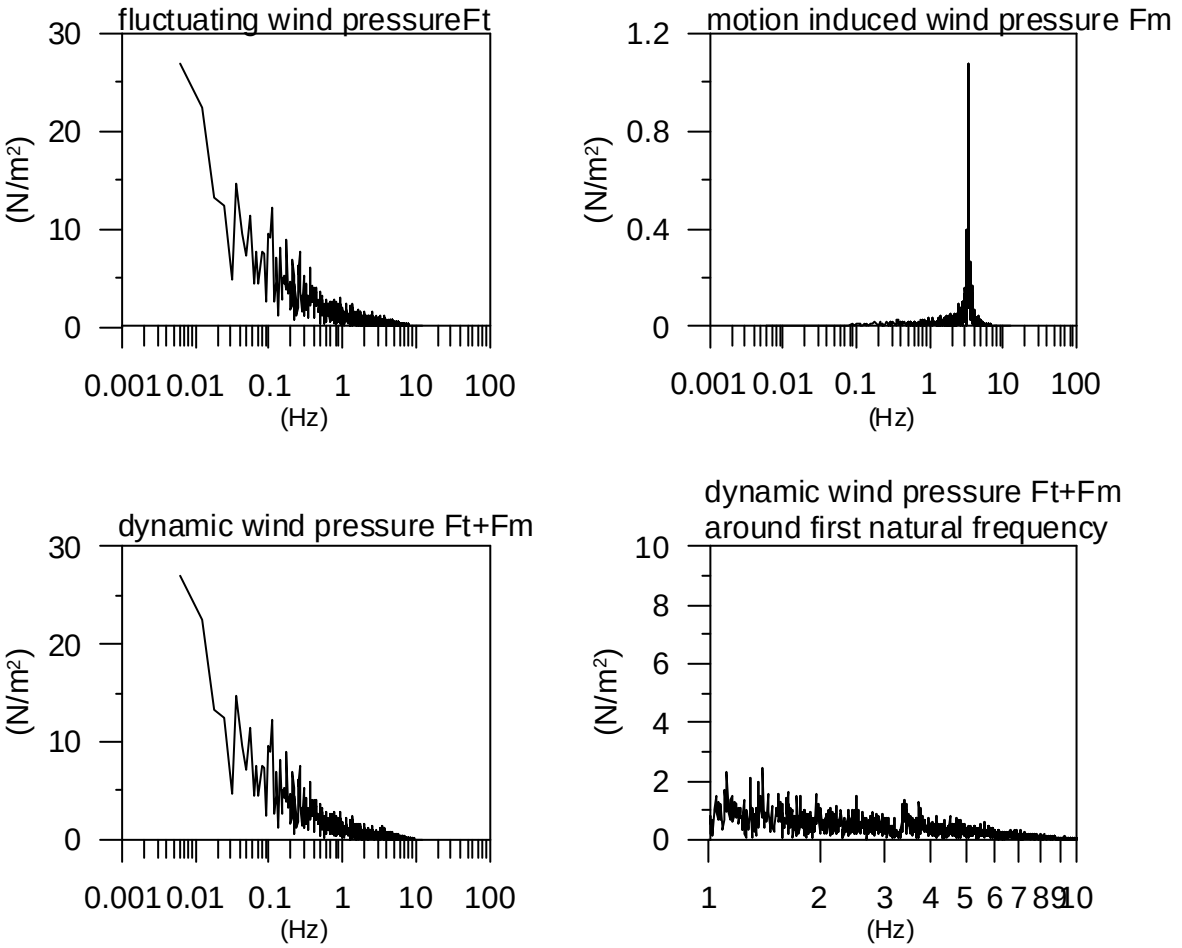

Fig.4.6 Fourier spectrum of fluctuating wind pressure, motion induced wind pressure, dynamic wind pressure (sum of fluctuating wind pressure and motion induced wind pressure) and the extension of the dynamic wind pressures graph
Glass plate B, point-support system, mean wind velocity 17m/s

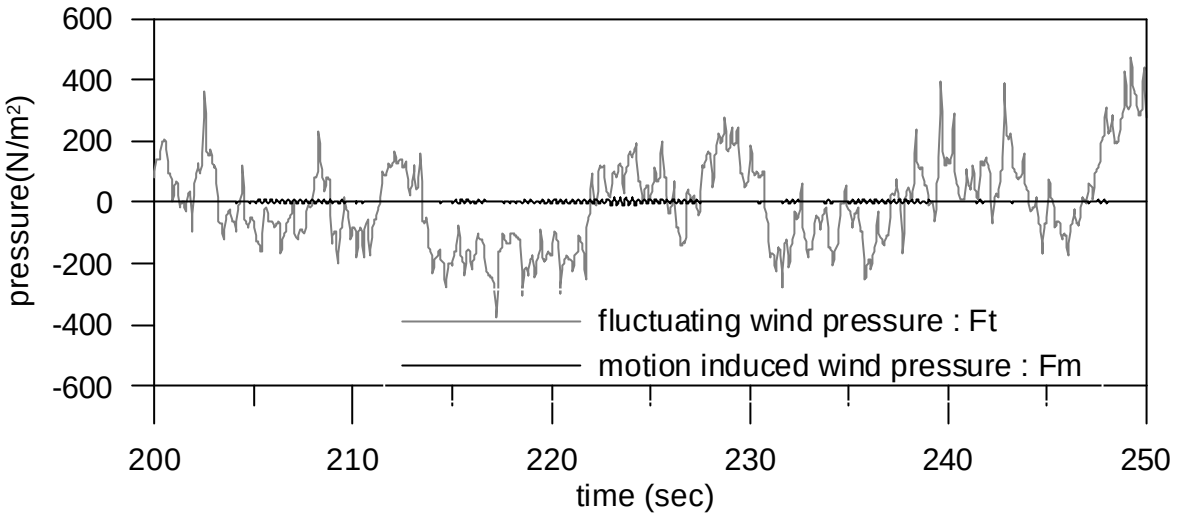

Fig.4.7 Time series of fluctuating wind pressure and motion induced wind pressure
Glass plate B, 4 line support, mean wind velocity 30m/s

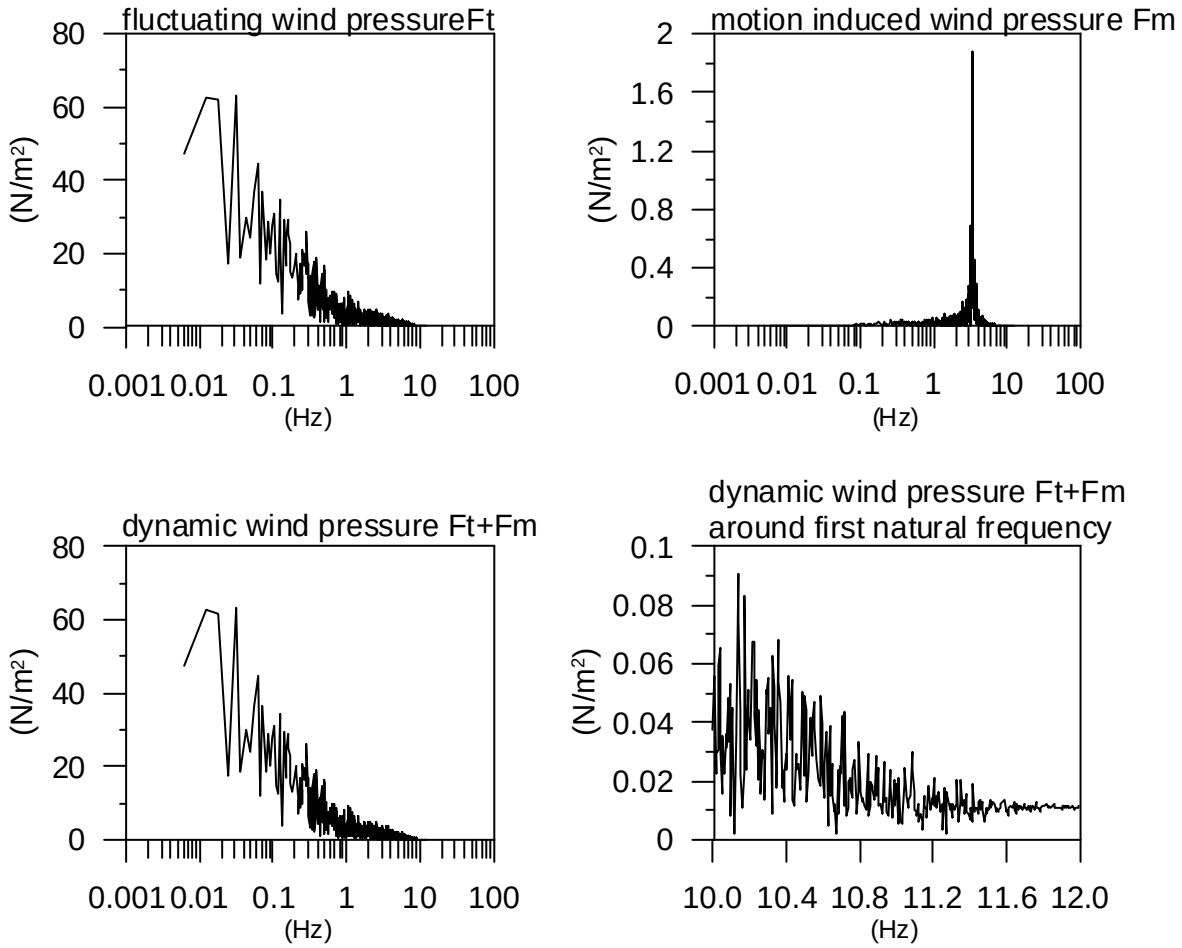

Fig.4.8 Fourier spectrum of fluctuating wind pressure, motion induced wind pressure, dynamic wind pressure (sum of fluctuating wind pressure and motion induced wind pressure) and the extension of the dynamic wind pressures graph
Glass plate B, 4 line-support system, mean wind velocity 30m/s

4.3 Discussion

In the Fig. 4.1, the time series of motion induced wind pressure and the fluctuating wind pressure under the 30m/s mean velocity wind are shown. The maximum value of the motion induced wind pressure F_m is 40 N/m^2 where as the maximum value of the fluctuating wind load (F_t) is about 400 N/m^2. The maximum value of F_m, 10% of the maximum value of F_t, is observed on the spectrum of the dynamic wind load (F_m+F_t) as a small peak at around the first natural frequency of 3.6 Hz.

Under the condition of the mean wind velocity of 24 m/s, the maximum value of the motion-induced wind load becomes less than 4 % of the maximum value of the fluctuating wind load. On the spectrum of the wind dynamic load, the peak at around the first natural frequency is much smaller than the peak observed in Fig. 4.2 of the spectrum of the dynamic wind load under the mean wind velocity of 30 m/s.

Furthermore, when the mean wind velocity of 17m/s, the peak around the first natural frequency is hardly recognized in the Fig. 4.6.

Only in case of a storm with the mean wind velocity of 30 m/s, which actually happens once in more than 50 years in accordance with the Eurocode, the dynamic wind load is influenced by the motion of the facade element.
Concerning the result of time series of the 4-line supported glass (Fig.4.7), motion induced wind load is not comparable to the fluctuating wind load.
From these results, the motion induced wind load can be ignored and it is assumed that, the fluctuating wind load is equal to the dynamic wind load on glass facade.

5 Loading-Cycle of Wind

5.1 Introduction

The tensile strength of glass is much smaller than the compressive strength. Therefore when discussing glass material, the tensile strength is important. The tensile strength in practice is much smaller than the theoretical value (theoretical value is 5000-10000N/mm^2, the practical value is around 30-100N/mm^2 for a normal float glass) [5.1], because of cracks developed on the glass surface. Generally fatigue of a material is progressed by the growing cracks. First an initial crack occurs on the surface. The crack results from surface scratches by handling or tooling of the material. Then the crack continues to grow due to repeating loads (Fig. 5.1).

In addition, glass is a brittle material that shows no plastic behavior. Therefore, glass can be broken very quickly without any previous signal. In the condition of a static load, the strength of glass is lowered as increase of loading time, whereas in the condition of dynamic load, the strength of glass is lowered in accordance with the decrease of the loading speed [5.2]. For further analysis on our study of the building structure with glass materials, a fatigue analysis of glass is essential.

It is clear that the main dynamic load that continuously acts on glass facade in its lifetime is caused by wind. For a fatigue analysis, loading-cycle of the wind in the lifetime is necessary to be identified. In this study, wind loading-cycles during the lifetime of a structure are counted by using probabilistic theories and a loading-cycle model is developed.

Fig. 5.1 Cracks developed on glass surface. Display extension ×100
Source: [5.1]

5.2 Fatigue Analysis

Before the wind loading-cycle counting, the general procedure of fatigue analysis is explained in Section 5.2. The procedure is used generally in the field of mechanical and civil engineering.

5.2.1 S-N Curve

The S-N curve (Wöhler-curve) is a practical tool to visualize time to failure for a material. The "S-N" means stress versus number of cycles to failure. In a S-N curve, the stress amplitude σ_a is plotted on the vertical axis and the logarithm of the number of cycle to failure N is on the horizontal axis. This S-N curve is obtained by a series of cycle loading test, in which a material is loaded by cyclic wave until the material fails. The S-N curve is material specific and each material has its own S-N curve. S-N curve typically consists of three parts. As an example, the S-N curves of steel and aluminum are shown in the Fig. 5.2.

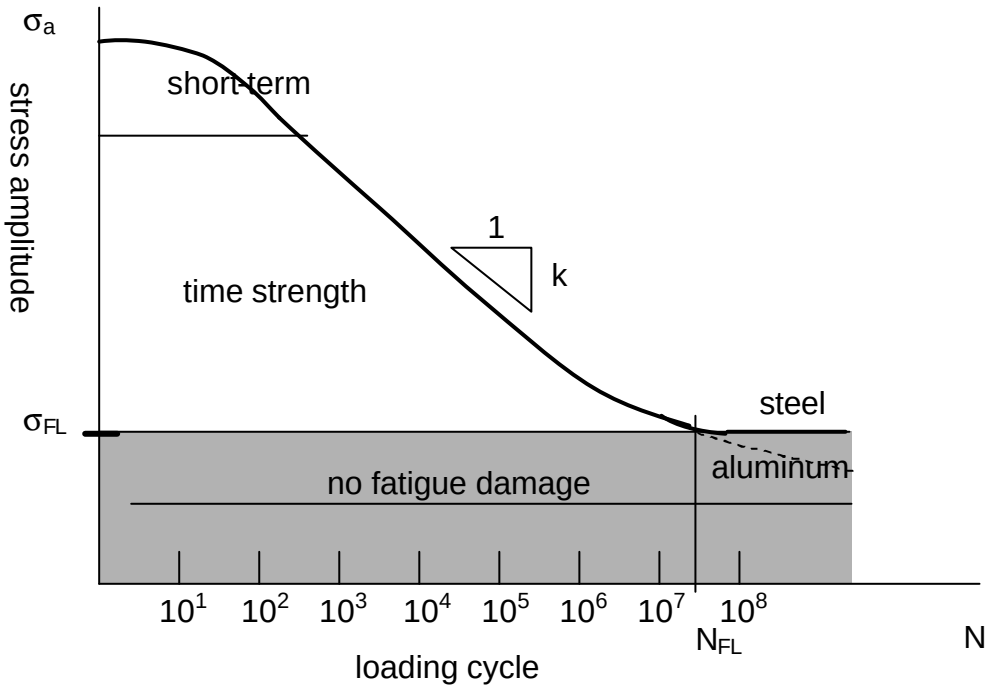

Fig. 5.2 Typical S-N curve

Short-term strength
At the high load-stress amplitude, the material fails in short time with lower cycle ($N=10^2$-10^4). This part of the S-N line is curved and non-linear.

Time strength
In the middle of the S-N curve, there is a nearly linear part. In this part, the relationship between loading-cycle to failure N and the amplitude of stress σ_a is expressed as:

$$N s_a^m = k \tag{5.1}$$

Fatigue strength
When the stress amplitude is lower than a certain value, no fatigue damage is induced, regardless the number of times of loading. For example, the stress limit σ_{FL} is around a loading-cycle $N_{FL}=2\times10^6$ for steel. The S-N curve of some materials, such as aluminum, copper and magnesium, do not reach "no fatigue zone", i.e, these materials must fail at some number of loading-cycles.

5.2.2 Loading-Cycle Counting

When the S-N curve of a material is known, the estimation of the fatigue failure of this material is possible with data of stress loading amplitude and the assumed loading-cycle of the external force. In reality, the load that act on a structure or structural part is random and dynamic. To estimate the fatigue failure, it is necessary to resolve the irregular time history into equivalent sets of block loading (loading-cycle model). In Fig. 5.3 the resolving process is shown.

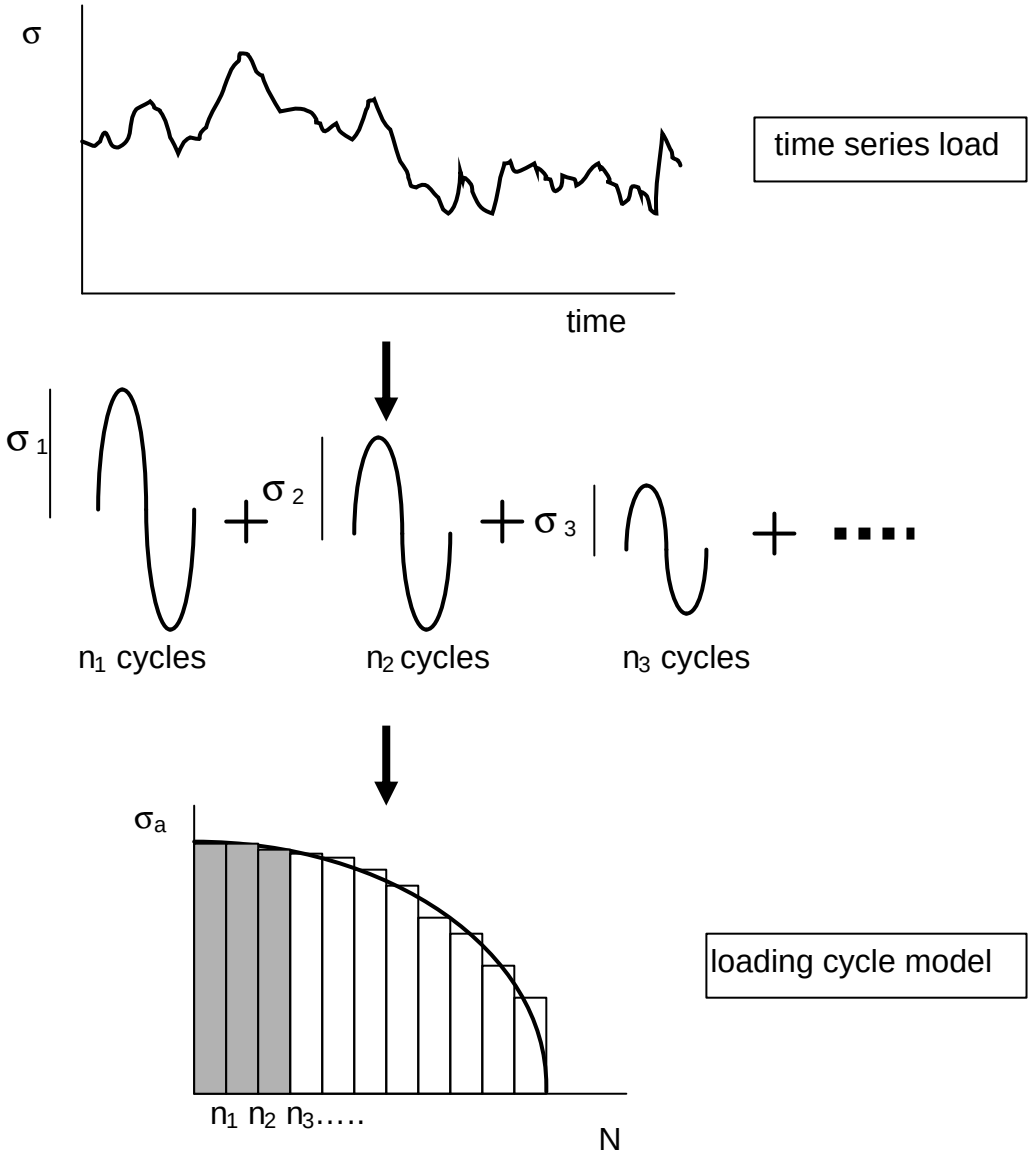

Fig. 5.3 Process to count loading-cycles and to produce a loading-cycle model

Rain-flow Counting

A method that is often applied to count loading-cycles is called rain-flow counting. The rain-flow counting is suggested to count dynamic loads in the mechanical field [5.5]. It is named "rain-flow" counting because the sketch of the counting method looks like a rain flow on a roof (Fig. 5.4).

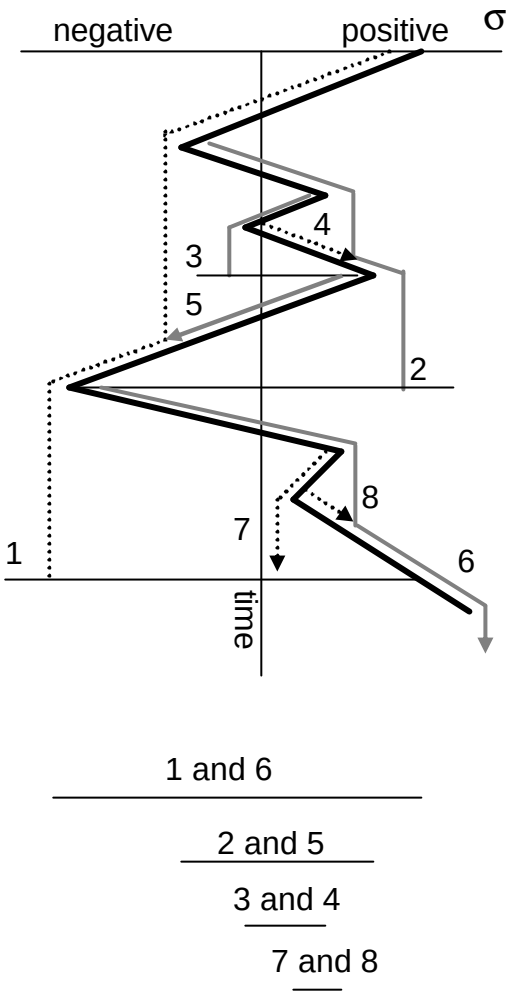

Fig. 5.4 Rain-flow counting method

The counting starts with a positive or negative peak and flows along the slope. The flow "drops" at the next smaller or larger peak and it stops in the following situations:

- When a flow started with a positive peak and stops if it passes a larger or equal size of positive peak
- When a flow started with a negative peak and stops if it passes a larger or equal size of negative peak
- When a flow reaches the path of another drop

In Fig. 5.4,

- Flow 1 passes an larger maximum
- Flow 2 passes a larger minimum
- Flow 3 passes a larger maximum
- Flow 4 reaches the run of drop 2
- Flow 5 reaches the run of drop 1
- Flow 6 falls down
- Flow 7 falls down
- Flow 8 reaches the run of drop 6

1 and 6, 2 and 5, 3 and 4 ; 7 and 8 form closed loops. Each loop is counted as a loading-cycle and the width of the loop becomes the amplitude.

5.2.3 Estimation of Fatigue Failure

From the S-N curve and the loading-cycle, the fatigue failure can be estimated. In Fig. 5.5, the loading-cycle model does not reach the S-N curve. The loading-cycle is smaller than the fatigue limit.

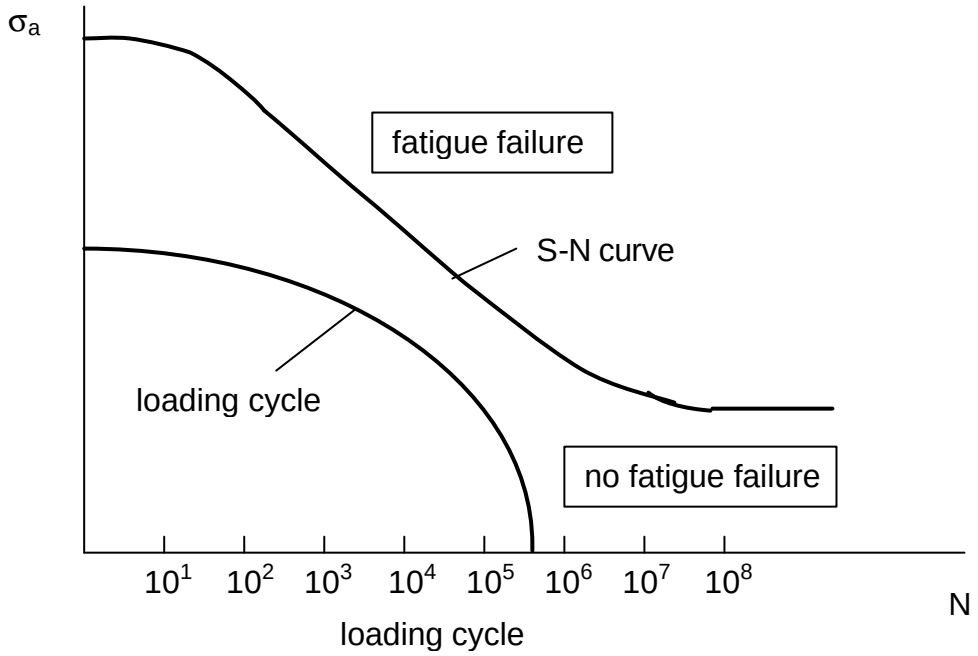

Fig. 5.5 Estimation of fatigue failure by SN-curve and loading-cycle

Palmgren – Miner Rule

To estimate fatigue failure for a material due to a dynamic load, the Palmgren–Miner rule is applied. According to the Palmgren – Miner rule, failure occurs when:

$$\sum_{i=1}^{I} \frac{ni}{Ni} \geq 1 \tag{5.2}$$

where n_i is the number of applied loading-cycle of type I, N_i is the pertinent fatigue life.

Now we assume that a material receives in its lifetime 500 times loading with amplitude a_1, 10^3 times with amplitude a_2 and 10^4 times with amplitude a_3. Using equation (5.2), the fatigue failure of this material is estimated :

$$\sum_{i=1}^{I} \frac{ni}{Ni} = \frac{500}{10^3} + \frac{10^3}{10^5} + \frac{10^3}{\infty} = 0.51 < 1 \tag{5.3}$$

In this case, the fatigue failure does not occur.

5.3 Loading-Cycle of Wind

The methods described in the last section are often used for the fatigue analysis. However when we apply the method to a glass facade under wind loads, the following problems may emerge :

- With a loading-cycle model, which is made by using the rain-flow method, the dynamic character of loading is not reflected well.

- When fatigue problems in the field of equipments or the fatigue of bridges caused by vehicles are discussed, the loads that structures or materials receive are generated by machines. Loads of machines are relatively constant during the service life time of the structures and it is not difficult to define a loading-cycle model that corresponds to the service life time load. However wind is a natural phenomenon and it is random. To define a loading-cycle model that corresponds to a service life time (usually 50 years) wind load, a probabilistic study is necessary.

In this study, loading-cycles that correspond in certain wind conditions are defined using a wind spectrum. Then a loading-cycle model which corresponds to 50 years loading-cycle is made by using the appearance probability of the wind condition.

5.3.1 Loading-Cycle Counting from Wind Spectrum

A random wave is considered as an aggregation of sine waves with different amplitudes and frequencies from a mathematical point of view. In DIN 4131 (see section 2.3.3), a certain frequency wave component (resonance frequency wave) is chosen and the loading-cycle of this wave during the service life time is counted. But in DIN 4131, the amplitude of the wave is not mentioned and only one frequency wave is pointed out. In this study, all ranges of frequency are taken and the loading-cycle of each frequency wave is counted.

Power spectrum density and amplitude

Power spectrum density $S(n)$ is defined such that $S(n)\times\Delta n$ expresses the amplitude ratio of an n to $n+\Delta n$ component wave. $S(n)\times\Delta n$ is a discrete spectrum and is called power spectrum. The power spectrum is expressed as :

$$S(n)\times\Delta n = 2\left|F(n)\right|^2 \tag{5.4}$$

where $F(n)$ is the Fourier spectrum and is usually a complex number. Fourier spectrum shows the component wave amplitude of frequency $n \sim n+\Delta n$. Mathematically, $|F(n)|$ is distributed from $-\infty$ to $+\infty$ but in the engineering field only positive values are taken and the amplitude a_n becomes :

$$a_n=2F(n) \tag{5.5}$$

then $a_n = \sqrt{2 \cdot \Delta n \cdot S(n)}$ is the amplitude of the $n \sim n+\Delta n$ frequency range wave.

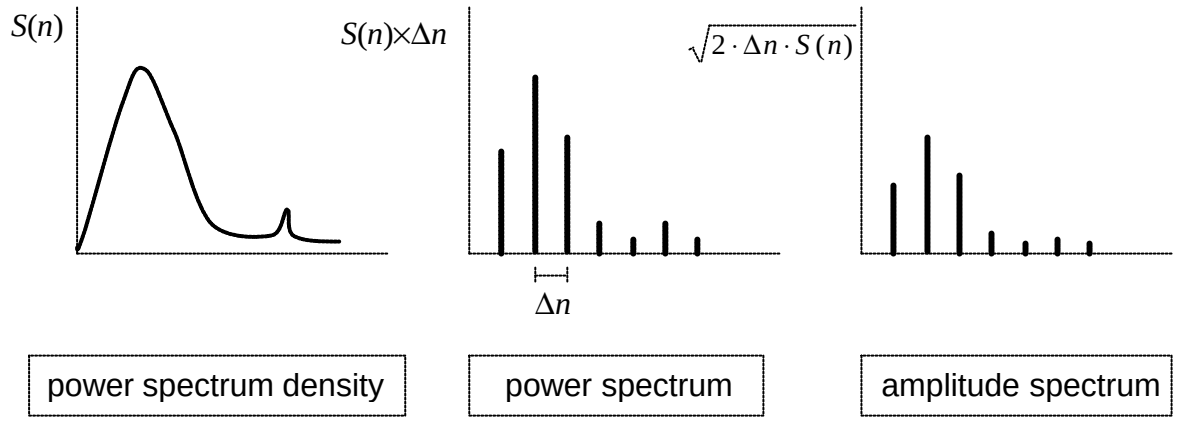

Fig. 5.6 Difference of power spectrum density, power spectrum and amplitude spectrum

The wind condition is assumed to be constant for 10 minutes. Now, the loading-cycle in 10 minutes is counted. If Δn is small enough, the frequency of a wave with amplitude a_n can be recognized as:

$$n+\frac{\Delta n}{2} \cong n \tag{5.6}$$

The loading-cycle of a wave component with the amplitude a_n and the frequency n (Hz) becomes $600(s) \times n$ (times/s).

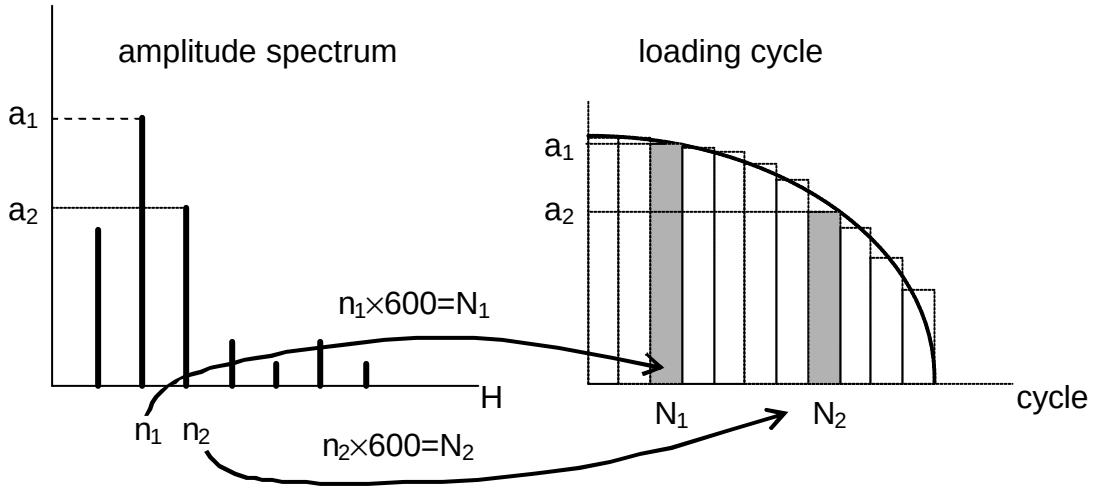

Fig. 5.7 Transformation form spectrum to loading-cycle

5.3.2 Probabilistic Study

After getting the loading-cycle model for a 10-minute span, the loading-cycle model which corresponds the service life time is calculated by using the appearance probability of the wind. As mentioned in 2.1.3, the appearance probability of the mean wind velocity fits to the Weibull distribution.

We assume that the appearance probability of a 10-minute mean wind velocity u is $p(u)$. From a loading-cycle model, which is calculated from a wind load spectrum of u m/s mean wind velocity, the loading-cycle of a load component with amplitude a_I is $N_s(u,i)$. Now, the loading-cycle of this wave during the service life of 50 years $N_{to}(u,i)$ is

$$N_{to}(u,\mathrm{i})=50\ \text{years}\times 365\ \text{days}\times 24\text{hours}\times 6\times N_s(u,i)\times p(u) \tag{5.7}$$

Note 6 in the equation means that 10-minute term appears 6 times in 1 hour.

The total loading-cycle in 50 years can be calculated by the equation (5.7), with each amplitude wave in each wind condition. The total loading-cycle N_{to} is

$$N_{to}=\sum_{u=1}^{U}\sum_{i=1}^{I}50\times 365\times 24\times 6\times N_s(u,i)\times p(u) \tag{5.8}$$

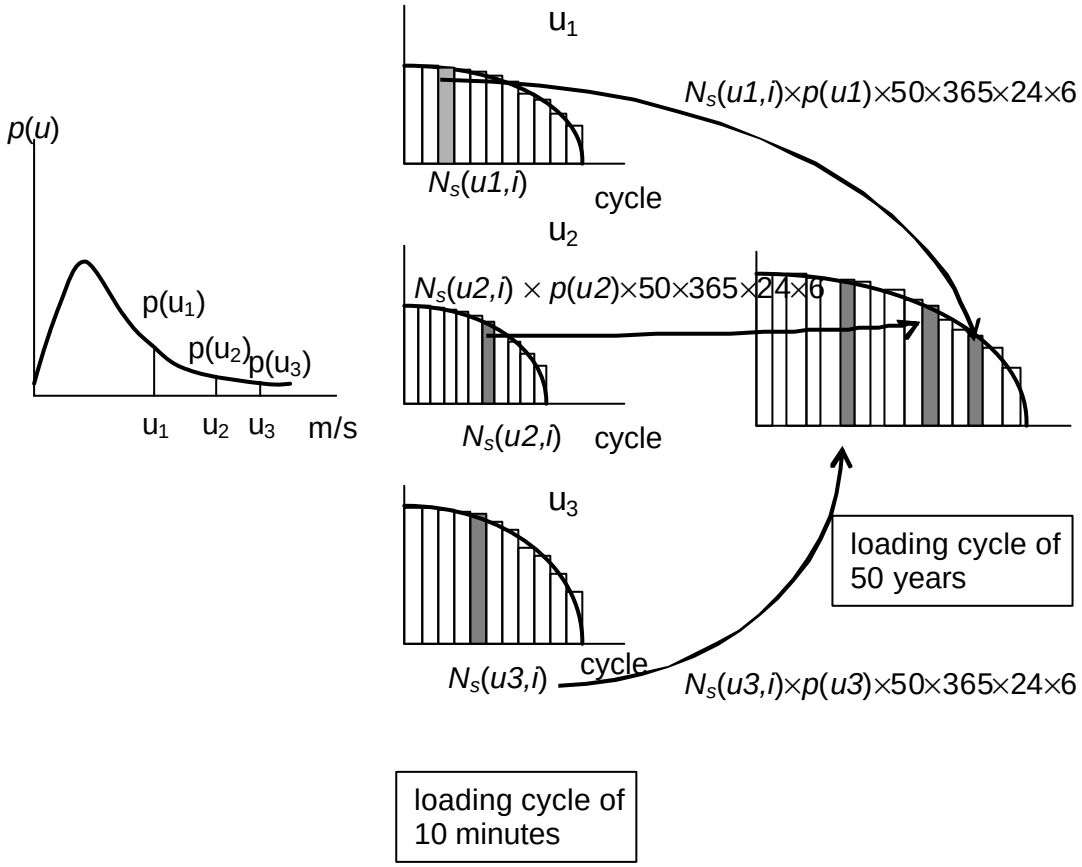

Fig. 5.8 Procedure of making loading-cycle model of a 50-year wind load

5.3.4 Calculation Results

The wind loading-cycle in 50 years service life time on glass facade is calculated by the method which is explained in the last section. With the result of the dynamic wind load on glass facade in Chapter 4, the natural fluctuation of wind can be considered as the dynamic wind load on glass facade. The wind loading-cycles are defined from the natural fluctuating wind spectrum.

We assume that the facades are located 20m and 50m high above the ground. The building is located in the urban area in Frankfurt and Hamburg. The Weibull parameters are obtained from the European Wind Atlas [5.6]. Probability density functions of wind velocity in Frankfurt and Hamburg at the height of 10m in urban area are shown in Fig. 5.9.

The calculation results are shown in the Fig. 5.10.

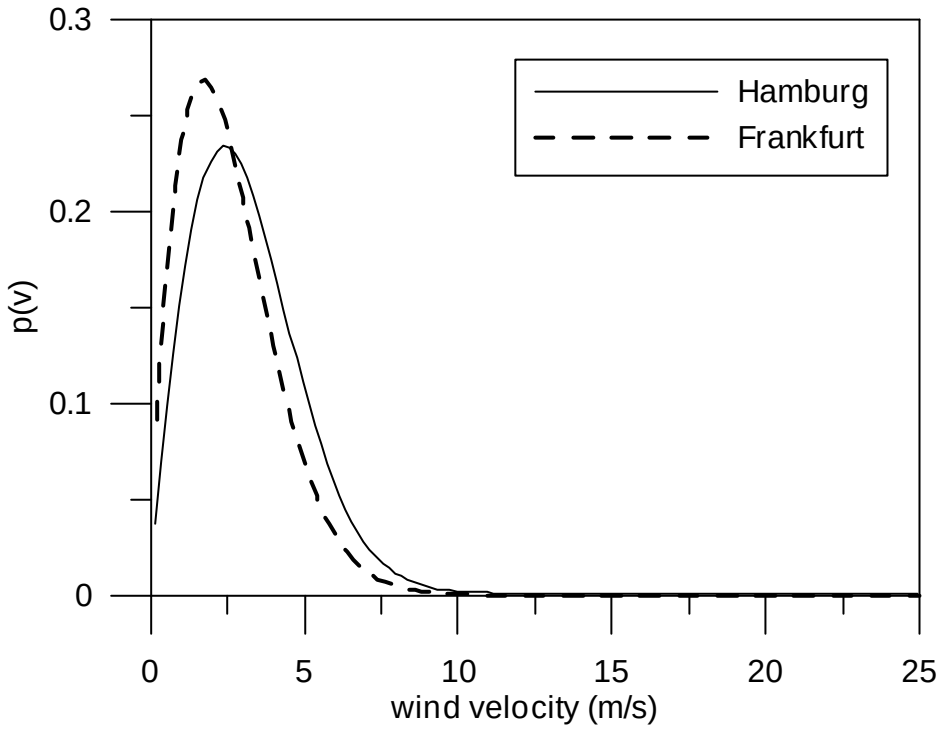

Fig. 5.9 Probability density functions of wind velocity in Hamburg and Frankfurt at the height of 10m, in urban area

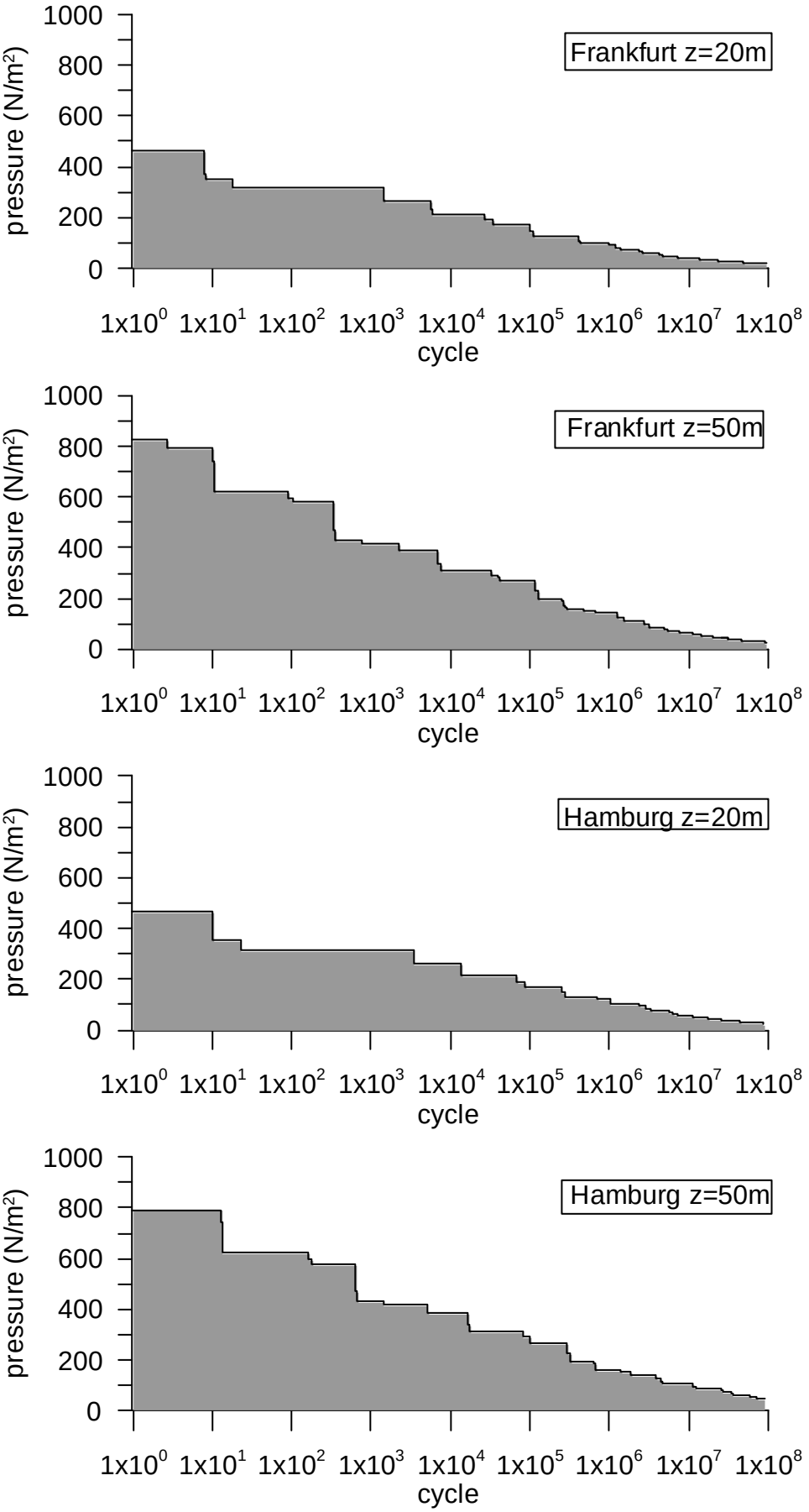

Fig. 5.10 Loading-cycle of 50 years wind in Frankfurt and Hamburg

5.3.5 Discussion

Concerning the loading-cycle model of at height of 20m, we can recognize the same tendency in both of Frankfurt and Hamburg. When the facade is located in Germany, the height of the glass facade shows a larger influence on the loading-cycle model than the location.

The loading-cycle models, which are shown in the last section, represent only the fluctuating part of the wind pressure. We need to take the mean value of the wind pressure into account. However, the mean wind pressure is not constant during the service life. How to take this values into the loading-cycle model is a difficult issue. For example, we can take a mean wind pressure that appears once in the service lifetime from the viewpoint of safety. Then, at the height of 50m in Hamburg, the mean wind pressure, the return period of which is 50 years, is $370\mathrm{N/m^2}$ and the pressure values in all loading-cycles move up to $370\mathrm{N/m^2}$ in *y* direction.

5.4 Reference

[5.1] Wörner, J. D., Schneider, J. and Fink, A. “Glasbau”, Springer, 2001

[5.2] Schneider, Jens “Festigkeit und Bemessung punktgelagerter Gläser und stoßbeanspruchter Gläser”, Dissertation of Darmstadt University of Technology, 2001

[5.3] Kerr, S.C., Russell, D.L., Patel, U.S. and Bishop, N.W.M. “FE- Based Wheel Fatigue Analysis Using MSC.FATIGUE” 1st MSC Worldwide Automotive Conference, Munich, 1999

[5.4] Radaj, Dieter “Ermüdungsfestigkeit”, Springer-Verlag, 1995

[5.5] Matsuishi, M. and Endo, T. “Fatigue of metals subjected to varying stress”, Japan Society of Mechanical Engineers Meeting, Fukuoka, 1968

[5.6] Troen, I. and Petersen, E.L., “European wind Atlas”, Riso, National Laboratory, Denmark 1989

6 Conclusion

In this study, the dynamic characters of glass facades were estimated and the vibration analysis of the glass facade under wind loading were performed. By using the analysis results, the dynamic wind load on glass facade was estimated. Then the loading cycle model which is necessary for a fatigue analysis was suggested by using probabilistic analysis.
The conclusions of this study are as follows.

- Natural frequency and natural form of a facade strongly depend on the area of the surface and the manner of the support. Specially the manner of the support has an influence on the sensitivity to the vibration. The vibration of the glass facade with point support system, which is popular in recent years, is large under the design level of wind velocity. For the design of a point supported glass facade, the danger of large vibrations must be reviewed.

- Spectrum of the motion-induced wind load has a peak around the natural frequency. However, the maximum value of the motion-induced wind load is approximately 10 % of the maximum value of the fluctuating dynamic load in time series. This value of the motion induced wind load appears only for the point supported facade under the extreme wind condition, such as a wind with a return period of 50 years. In other cases, the value of the motion-induced wind load is not comparable with the fluctuating wind load and can be ignored. If a larger value of the motion induced wind load is monitored, in the case, deformation of the glass plate is quite large. In such situation, the danger of failure of the glass due to a instant large tension is a larger problem than the large motion-induced wind load.

- A new method to count the loading-cycle of the wind is suggested. In the method, the spectrum of the fluctuating wind is pointed out and the loading cycles of each frequency components are counted. In the calculation cases that are carried out in this study, the resonance effect is very small. However, when the resonance component is large in the spectrum of the total wind load spectrum, this method is very effective.

- It is considered that an extreme wind period lasts 10 minutes. Loading-cycle counting in a extreme condition has been done in some studies. In this study, the total wind loading cycle in a life time of a structure is counted by taking the probabilistic theory into consideration. For the estimation of fatigue failure of a glass plate, we need also the S-N curve, the manner of the support and the area of the glass plate are necessary. A necessary data for the fatigue analysis were derived in this study.

Loading-cycle models on glass facade were suggested in this study. However parameters that characterize the fluctuating wind are different in some references and codes. Measured values

of turbulence intensities in urban areas are also not consistent. This indefiniteness must be considered when producing the dynamic wind numerically.

In this study, the model facades are single sheet glass and located on the weather side of the building. As mentioned in Chapter 2, the aero flow is disturbed by the building. Around the corners or on the back side of the building the spectrum of pressure is different from that of the front side. At these areas, the mean value of wind pressure is considered to be lowered. However, higher frequency components can be included in the spectrum because of the vortex shedding. In such situation, there is a possibility of a resonance between the high frequency component of the wind and the facade element. The aero flow is changed by the shape, the size and the surrounding condition of the structure. It is an interaction problem between air and structure. To estimate the wind velocity or the dynamic wind pressure at the corner or on the back side of the structure by analytical or numerical method is not convenient until now. When it will be easier to get these values in the future, the loading cycle counting with the consideration of the corner or backward of the building makes sense.

There are some problems because of the complicated system of glass facades in recent years. For example, concerning double facade, the resonance problem between two sheets of glass and the air in between is pointed out.

Each glass sheet is connected with the support system. When many plates of glass are considered as one large glass wall, the natural frequency is low and the possibility of the vibration with the natural wind becomes larger.

There are many of the problems of glass facades and wind or air. The loading cycle model which is derived in this study is only one suggestion. However, the analysis method which is developed in this study can be applied to the phenomena mentioned in this section. When these problems are solved in the future, more reasonable loading cycle model can be developed and it is very valiant for fatigue analysis of glass facade.

Appendix A Fourier Transform

A-1 Fourier Transform

The Fourier transform (FT) is a tool for transforming a signal in the time domain into the frequency domain (or the Fourier inverse transform transforms the signal in the frequency domain into the time domain). The Fourier transform F(n) of a continuous time function f(t) can be expressed as

$$F(n) = \int_{-\infty}^{\infty} f(t) \cdot e^{-i2\pi nt} dt \tag{A.1}$$

The inverse transform is

$$f(t) = \int_{-\infty}^{\infty} F(n) \cdot e^{-i2\pi nt} dn \tag{A.2}$$

A-2 Discrete Fourier Transform

The Fourier transform treats continuous function of $f(t)$ and $F(n)$. However, for computer analysis, the Fourier transform must be applied to a discrete complex valued series.

Consider a complex series x(k) with N samples of the form

$$x_0, x_1, x_2, x_3 \ldots k \ldots x_{N-1} \tag{A.3}$$

where x is a complex number

$$x_i = x_{real} + j\, x_{imag} \tag{A.4}$$

Further, assume that the series outside the range 0, N-1 is extended N-periodic, that is, $x_k = x_{k+N}$ for all k. The FT of this series will be denoted X(k), it will also have N samples. The forward transform will be defined as :

$$X(n) = \frac{1}{N} \sum_{k=0}^{N-1} x(k) e^{-jk2\pi n/N} \qquad \text{for } n=0 \ldots N-1 \tag{A.5}$$

The inverse transform will be defined as :

$$x(n) = \sum_{k=0}^{N-1} X(k) e^{jk2pn/N} \qquad \text{for } n=0\ldots N\text{-}1 \qquad \text{(A.6)}$$

A-3 Fast Fourier Transform

The fast Fourier transform (FFT) is simply a kind of the discrete Fourier transform (DFT), which saves computational time by special algorithms.

The only requirement of the most popular implementation of this algorithm is that the number of points in the series be a power of 2. The computing time for the FFT is proportional to

$$N \log_2(N) \qquad \text{(A.7)}$$

For example a transform on 1024 points using the DFT takes 10 times longer than using the FFT, a significant speed increase. Note that in reality comparing speeds of various FFT routines is problematic, many of the reported timings have more to do with specific coding methods and their relationship to the hardware and operating system.

Acknowledgements

I wish to thank Prof. Dr.-Ing. Johann-Dietrich Wörner for his encouragement and constant interest throughout my research. I am extremely grateful for his vast knowledge of dynamics in structural engineering and his leadership.

I would like to thank Prof. Dr. Ing. Ulrich C. E. Zanke for taking on the task of examiner. His interest in my research, advice and daily kindness during my research time are also sincerely acknowledged.

My dissertation was sponsored by the State of Hesse through the program of Graduate Scholarship. This financial support is gratefully acknowledged.

I must also thank the group I had the pleasure of working with over the last two years.

Lastly, I thank very deeply my parents. Without their generous help, this work would not have been possible.

Darmstadt, May 2003

Yukako Nakagami